Inhalation Toxicology
International Forum for Respiratory Research

ISSN: 0895-8378 (Print) 1091-7691 (Online) Journal homepage: http://www.tandfonline.com/loi/iiht20

Pulmonary toxicity following acute coexposures to diesel particulate matter and α-quartz crystalline silica in the Sprague-Dawley rat

Breanne Y. Farris, James M. Antonini, Jeffrey S. Fedan, Robert R. Mercer, Katherine A. Roach, Bean T. Chen, Diane Schwegler-Berry, Michael L. Kashon, Mark W. Barger & Jenny R. Roberts

To cite this article: Breanne Y. Farris, James M. Antonini, Jeffrey S. Fedan, Robert R. Mercer, Katherine A. Roach, Bean T. Chen, Diane Schwegler-Berry, Michael L. Kashon, Mark W. Barger & Jenny R. Roberts (2017) Pulmonary toxicity following acute coexposures to diesel particulate matter and α-quartz crystalline silica in the Sprague-Dawley rat, Inhalation Toxicology, 29:7, 322-339, DOI: 10.1080/08958378.2017.1361487

To link to this article: http://dx.doi.org/10.1080/08958378.2017.1361487

Published online: 01 Oct 2017.

INHALATION TOXICOLOGY, 2017
VOL. 29, NO. 7, 322–339
https://doi.org/10.1080/08958378.2017.1361487

Taylor & Francis
Taylor & Francis Group

RESEARCH ARTICLE

Pulmonary toxicity following acute coexposures to diesel particulate matter and α-quartz crystalline silica in the Sprague-Dawley rat

Breanne Y. Farris[a,b], James M. Antonini[a,c], Jeffrey S. Fedan[a,b,c], Robert R. Mercer[a], Katherine A. Roach[a,c], Bean T. Chen[a], Diane Schwegler-Berry[a], Michael L. Kashon[a], Mark W. Barger[a] and Jenny R. Roberts[a,b,c]

[a]National Institute for Occupational Safety and Health, Morgantown, WV, USA; [b]School of Medicine, West Virginia University, Morgantown, WV, USA; [c]School of Pharmacy, West Virginia University, Morgantown, WV, USA

ABSTRACT

The effects of acute pulmonary coexposures to silica and diesel particulate matter (DPM), which may occur in various mining operations, were investigated *in vivo*. Rats were exposed by intratracheal instillation (IT) to silica (50 or 233 μg), DPM (7.89 or 50 μg) or silica and DPM combined in phosphate-buffered saline (PBS) or to PBS alone (control). At one day, one week, one month, two months and three months postexposure bronchoalveolar lavage and histopathology were performed to assess lung injury, inflammation and immune response. While higher doses of silica caused inflammation and injury at all time points, DPM exposure alone did not. DPM (50 μg) combined with silica (233 μg) increased inflammation at one week and one-month postexposure and caused an increase in the incidence of fibrosis at one month compared with exposure to silica alone. To assess susceptibility to lung infection following coexposure, rats were exposed by IT to 233 μg silica, 50 μg DPM, a combination of the two or PBS control one week before intratracheal inoculation with 5×10^5 *Listeria monocytogenes*. At 1, 3, 5, 7 and 14 days following infection, pulmonary immune response and bacterial clearance from the lung were evaluated. Coexposure to DPM and silica did not alter bacterial clearance from the lung compared to control. Although DPM and silica coexposure did not alter pulmonary susceptibility to infection in this model, the study showed that noninflammatory doses of DPM had the capacity to increase silica-induced lung injury, inflammation and onset/incidence of fibrosis.

ARTICLE HISTORY
Received 20 April 2017
Revised 15 June 2017
Accepted 26 July 2017

KEYWORDS
Crystalline silica; diesel exhaust particulate matter; immune response; occupational exposure; pulmonary fibrosis

Introduction

The natural gas and oil industry is one of the most rapidly growing industries in the United States. Specifically, the industry is expanding in the area of hydraulic fracturing, "fracking," or horizontal drilling. This process extracts natural resources from otherwise inaccessible deposits below the earth's surface, provided more than two million jobs in 2012 and is estimated to support approximately four million jobs by 2025 (API, 2014). Two respirable particulates identified as possible exposure hazards in fracking workplaces include diesel particulate matter (DPM) and α-quartz crystalline silica (SiO_2) (Breitenstein et al., 2011). These two particulates are also present in combination in other mining operations including below ground mining operations, particularly in coal extraction. Although toxicity of these two particulates have been studied in detail as individual exposures, there are currently no *in vivo* studies, as far as we are aware, that have examined the pulmonary effects of the particulates in combination at doses that are relevant to various mining operations.

In addition to underground mining operations and operations in hydraulic fracturing, where significant numbers of diesel engines are utilized (transport, drilling and pumping), diesel exhaust (DE) exposure is also prevalent in industries including trucking and railroad operations (OSHA/MSHA, 2013). DE is a highly complex mixture of chemical substances but is primarily composed of an elemental carbon (EC) core having additional organic carbon constituents adsorbed to it. Other than the EC components, compounds typically contained in DE include: polyaromatic hydrocarbons (PAHs), sulfates, silicates, nitrates, as well as metallic particulates (OSHA/MSHA, 2013). DPM exposure is linked to a variety of adverse health outcomes, including enhanced sensitization to allergic stimulus, development and aggravation of asthma, chronic bronchitis, decreased lung function, airway inflammation, decreased vascular function and development of cancers, as reported in epidemiological studies (Beatty & Shimshack, 2011; Diaz-Sanchez et al., 1999; Gauderman et al., 2004; Garshick et al., 2004; Kachuri et al., 2016; Lucking et al., 2011; McCreanor et al. 2007; Nightingale et al., 2000). Based on these studies, DE and DPM have been identified by the International Agency for Cancer Research (IARC) as a group 1 carcinogen (IARC, 2012; OSHA/MSHA, 2013). In addition to human cohort studies, studies involving healthy human volunteers exposed to DE/DPM in a controlled chamber have also shown that DE/DPM caused pulmonary inflammation in acute exposure scenarios (Nightingale et al., 2000; Salvi et al., 1999). Controlled human studies as reviewed by Ghio et al. (Ghio

CONTACT Breanne Y. Farris wcq0@cdc.gov CDC/NIOSH/HELD, 1095 Willowdale Rd., MS4020, Morgantown, WV, 26505, USA

et al., 2012a,b) show that inflammation occurs in the respiratory tract of humans exposed to DPM and that this occurs in a dose-dependent manner. DPM toxicity has also been investigated *in vivo* and *in vitro*. DPM has been shown to enhance airway reactivity, inflammation, production of reactive oxygen species (ROS) and increased development and severity of allergic asthma, lung fibrosis, lung injury, alveolar edema, lung cancer and mortality in exposed animals (Brandt et al., 2013, 2015; Ichinose et al., 1995; Kim et al., 2016; Ma & Ma, 2002; Madden et al., 2000; Mauderly et al., 1994; Sagai et al., 1993; Singh et al., 2004; Zhao et al., 2009). Studies conducted *in vitro* suggest, similarly, that DPM contributes to airway inflammation, production of reactive oxidants, unfolded protein response, allergic response, decreased mucociliary clearance and upregulation of cancer-associated proteins in lung cells (Abe et al., 2000; Bayram et al., 1998; Jung et al., 2007; Le Vee et al., 2016; Ohtoshi et al., 1998; Sagai et al., 1993, 1996; Totlandsdal et al., 2015; Vattanasit et al., 2014; Zhou et al., 2015). Furthermore, DPM has been shown to alter the pulmonary immune function and is associated with increased susceptibility to infection (Castranova et al., 2001; Ma & Ma, 2002; Mundandhara et al, 2006; Pierdominici et al., 2014; Provoost et al., 2010; Siegel et al., 2004; Steerenberg et al., 1998; Yin et al., 2002).

Several countries have regulations to control occupational exposure to DE or DPM. These regulations vary relative to underground mining operations versus above-ground mining and nonmining workplaces. In addition, exposure is differentially regulated by DE constituents (total particle, elemental carbon, nitrogen) (HSE, 2012; QDNRM, 2014; OSHA/MSHA, 2013; SUVA, 2013). In the United States, recommended exposure limits (REL) exist for many of the components of DE as individual emissions; however, there is currently no Occupational Safety and Health Administration (OSHA) regulation of DPM in nonmining, occupational settings. The Mine Safety and Health Administration (MSHA) REL for DE and DPM in underground mine operations is a time-weighted average (TWA), based on an 8-h work day, of 160 $\mu g/m^3$ total carbon, which includes DPM as elemental carbon. Additionally, the California Department of Health Services (CDHS) has recommended an occupational exposure limit (OEL) of 20 $\mu g/m^3$ elemental carbon (CDHS, 2002). Both Switzerland and Australia have set OELs at 100 $\mu g/m^3$ elemental carbon (QDNRM, 2014; TERA, 2014).

Workplace exposure to SiO_2 also occurs in a multitude of occupations and are well documented for a variety of mining operations, as well as in masonry, painting, sand blasting, construction, demolition and ceramics (Beckett et al., 1997; Yassin et al., 2005). SiO_2 is one of the most common minerals occurring in the earth's crust and is a major component of sand. Sand that contains SiO_2 is the primary proppant, or substance used to stabilize the fracture during hydraulic fracturing operations and subsequent resource extraction. A respirable fraction of this sand can become airborne when transported onto/around fracking sites or pumped at high volumes/pressure into the well-bore (Esswein et al., 2013). The respiratory toxicity of the crystalline form of SiO_2 is well-established, and therefore, OSHA requires workplaces to follow the permissible exposure limits (PEL) set at 0.05 mg/m^3 as a TWA for respirable crystalline SiO_2. Inhalation of respirable SiO_2 has been shown to cause lung inflammation and injury, chronic obstructive pulmonary disorders, bronchitis, emphysema, fibrosis, silicotic pneumoconiosis, cancer, heart disease, autoimmune disorders and increased risk of infection in humans (Beckett et al., 1997; Hnizdo, 2003; Kachuri et al., 2014; Liao et al., 2015; Liu et al., 2014; Maciejewska, 2014; Madl et al., 2008), depending upon duration and level of exposure.

Further, *in vivo* studies of SiO_2 exposure have investigated the mechanisms associated with pathologies, such as fibrosis and cancer, including chronic inflammation and the upregulation of acute inflammatory mediators like leukotriene B_4, upregulation of the NF-κB pathway, increased oxidant burden attributable to both the presence of free radicals associated with particles and oxidant production by cells in response to SiO_2 exposure, upregulation of genes associated with mucus production and pulmonary toxicity and activation of the inflammasome (Cassel et al., 2008; Kawasaki, 2015; Porter et al., 2002; Satpathy et al., 2015; Sellamuthu et al., 2013; Vallyathan et al., 1995). *In vitro* studies have shown production of oxidants and inflammatory mediators, activation of cell-signaling pathways associated with cancer, damage to DNA, and increased expression of genes related to inflammation, apoptosis, cancer and fibrosis in response to SiO_2 exposure (Gwinn et al., 2009; Ovrevik et al., 2004; Sellamuthu et al., 2011; Shi et al., 1995; Tomaru & Matsuoka, 2011; Vallyathan et al., 1992), furthering support for mechanisms underlying the pathologies observed in animal models of disease related to occupational exposure. SiO_2 exposure has also been implicated in the alteration to the immunological environment in the respiratory tract (Huaux et al., 1998; Langley et al., 2004) and contributions to respiratory susceptibility to some infections (Beamer & Holian, 2008; Pasula et al., 2009).

While the pulmonary toxicity to constituents of diesel, and SiO_2 are well studied as individual exposures, little is known about the effects these particles may have when encountered as a mixed exposure. Mining operations including hydraulic fracturing for oil or gas, as well as above- and below-ground metal/nonmetal-mining operations, are environments where workers may be exposed to constituents of diesel and SiO_2 simultaneously, rendering it paramount to establish whether coexposure to these particles will enhance or alter pulmonary toxicity. The current study was designed to investigate the hypothesis that combined exposures to these particles would result in amplified injury, inflammation and cellular recruitment to the lung in an acute exposure scenario. Additionally, our study addressed whether or not cell-mediated clearance of a pathogen would be altered by the coexposure. Existing *in vivo* and *in vitro* studies documenting the toxicity of DPM or SiO_2 *in vivo* often examine doses of these materials representative of chronic exposures or doses that exceed typical workplace exposures in single bolus doses (Creutzenberg et al., 2008; Ghio et al., 1994; Kajiwara et al., 2007; Ma et al., 2014; Robertson et al., 2012; Yang et al., 2001). Therefore, doses for the current study were based on field measurements of SiO_2 taken during

active above-ground mining operations (Esswein et al., 2013). Values for diesel were derived from both underground mining values (McDonald et al., 2002; Pronk et al., 2009) for high-dose values and from existing OELs for elemental carbon for the lower dose (SUVA, 2013; OSHwiki Contributors, 2017; TERA, 2014). A single acute bolus dose of silica, diesel particulate, or a combination of the particles at different doses were administered to Sprague-Dawley rats by intratracheal instillation. Lung injury, inflammation and immune responses were evaluated over a three-month time course. Additionally, alteration in susceptibility to pulmonary infection following exposure to the particles in combination was evaluated to further assess alterations in immune response.

Methods

Particles

Particles in these studies are used as surrogates to represent work site exposures. DPM was obtained from the National Institute of Standards and Technology (NIST) as a commercially available NIST Standard Reference Material (SRM) 2975 (referred to as DPM in the study). SRM 2975 was originally collected from an industrial forklift in the 1990s (Certificate of Analysis Standard Reference Material 2013, 2975). The surrogate particle used for SiO_2 is α-quartz crystalline silica (SIL; MIN-U-SIL® 5, US SILICA; Berkeley Springs, WV).

Dose determination

Doses were derived from field measurements of particles and applied to the equation below (EQ1) to quantify the amount of particle that would deposit in the lung of an average male worker doing moderate work (31.3% sitting and 68.8% light exercise) for 12 h per day for a period of 14 continuous days using a pulmonary deposition efficacy for each particle derived using a software-based algorithm (LUDEP 2.0) that considers particle characteristics including mass median aerodynamic diameter and geometric standard deviation, as well as shape and density (ICRP, 1994). These doses were then normalized to the surface area of both the worker's and the rat's lungs to obtain doses for *in vivo* studies (EQ2). DPM estimated as elemental carbon was reported to be variable depending on operations at hydraulic fracturing sites; (personal communication with JS related to Esswein et al., 2013; unreferenced) however, it was generally below the MSHA recommendation of 160 μg/m^3 total carbon (120 μg/m^3 elemental carbon equivalent), and DPM in underground mining operations has been measured in excess of 500 μg/m^3 as elemental carbon as reviewed by Pronk et al. (2009). Therefore, in this study, two doses of DPM were evaluated. The low dose (7.89 μg per rat) was derived from the OELs for DPM measured as elemental carbon of 100 μg/m^3 TWA (0.100 μg/L) (EQ3). The high dose of DPM was derived from high elemental carbon-level measurements taken during underground mining of 637 μg/m^3 (0.637 μg/L) (EQ4) (McDonald et al., 2002).The SiO_2 high dose (233 μg SIL) was derived from the highest SiO_2 levels measured during hydraulic fracturing site visits (Esswein et al., 2013), 2.5 mg/m^3 (2.5 μg/L) (EQ5). In addition, to assess exposure to equivalent doses of both particles at a less toxic dose of SIL, 50 μg of SIL was also evaluated as the low dose of SIL.

EQ1 – Basic equation for standard worker lung deposition:

$$\begin{aligned}&=(\text{field concentration, } \mu g/l)\\&\times (\text{minute ventilation, } l/\text{min})\\&\times (\text{exposure time per day, } \text{min}/d)\\&\times (\text{total fracking days, } d)\\&\times (\text{pulmonary deposition efficacy, unitless})\end{aligned}$$

EQ2 – Equation for normalization to rat lung surface area:

$$\begin{aligned}&=(\text{worker's deposited dose}/\\&\quad \text{average male worker lung surface area})\\&\times (\text{average rat lung surface area})\end{aligned}$$

EQ3 – Equation for low DPM dose:

$$\begin{aligned}&\text{Worker lung deposition} = (0.10\ \mu g/l) * (20\ l/\text{min})\\&\quad *(720\ \text{min/day}) * (14\ \text{days}) * (0.10) = 2016\ \mu g\\&\text{Dose calculated} = (2016\ \mu g/102.2m^2)\\&\quad *(0.4m^2) \approx 7.89\ \mu g\ \text{per rat}\end{aligned}$$

EQ4 – Equation for high DPM dose:

$$\begin{aligned}&\text{Worker lung deposition} = (0.637\ \mu g/l) * (20\ l/\text{min})\\&*(720\ \text{min/day}) * (14\ \text{days}) * (0.10) \approx 12,842\ \mu g\\&\text{Dose calculated} = (12,842\ \mu g/102.2m^2)\\&*(0.4m^2) \approx 50\ \mu g\ \text{per rat}\end{aligned}$$

EQ5 – Equation for high SIL Dose:

$$\begin{aligned}&\text{Worker lung deposition} = (2.5\ \mu g/l) * (20\ l/\text{min})\\&*(720\ \text{min/day}) * (14\ \text{days}) * (0.118) = 59,472\ \mu g\ \text{per worker}\\&\text{Dose calculated} = (59,472\ \mu g/102.2m^2)\\&*(0.4m^2) \approx 233\ \mu g\ \text{per rat}\end{aligned}$$

DPM and SIL preparation and characterization

Particles were prepared in USP-grade phosphate-buffered sterile saline (PBS) without Ca^{2+} or Mg^{2+} (AMERESCO; Solon, OH) for intratracheal instillation. A sonication process was used to disperse agglomerated particles. DPM was prepared as a 2 mg/mL stock solution and SIL was prepared as a 10 mg/mL stock solution, vortex mixed for one min, followed by 1 min of continuous sonication (GE130PB ultrasonic processor; General Electric, Boston, MA). Aliquots of stock solution were then further diluted to: 7.89 μg DPM, 50 μg DPM, 50 μg SIL, 233 μg SIL, 7.89 μg DPM +233 μg SIL, 50 μg DPM +50 μg SIL or 50 μg DPM +233 μg SIL in 0.3 mL PBS. Particles were then vortex mixed for an additional 30 s, followed by 15 s of sonication prior to intratracheal instillation. Particle preparations were dried onto filters and evaluated by field emission scanning electron microscopy (FESEM) to determine particle size. Energy-

dispersive X-ray (EDX) was performed to determine the elemental components of the particles as a measure of particle purity. The DPM was comprised primarily of the carbonaceous core, or EC of diesel, with very little detectable trace elements including: chromium, copper, iron, nickel, oxygen, silicon and zinc. Due to their volatile nature, PAHs cannot be measured using EDX, but the total extractable mass including the certified mass fractions of PAHs contained in NIST SRM 2975 is given as 2.7% of the total sample as described in the certificate of analysis (Certificate of Analysis Standard Reference Material 2013, 2975). No trace metals were detected in the SIL sample.

Animals

Male Sprague-Dawley [Hla:(SD) CVF] (SD) rats from Hilltop Lab Animals (Scottdale, PA), weighing approximately 300 g and free of viral pathogens, parasites, mycoplasmas, *Helicobacter* and CAR *Bacillus*, were used for all studies. Rats were housed in the pathogen free, environmentally controlled, Association for Assessment and Accreditation of Laboratory Animal Care International (AAALAC)-accredited facility. The rats were housed in ventilated polycarbonate cages, two per cage, on Alpha-Dri cellulose chips and hardwood Beta chips as bedding; they were provided HEPA-filtered air, irradiated Teklad 2918 diet, and tap water ad libitum; and were allowed to acclimate for one week before exposure. Rats were not restricted from enrichment activity (i.e. chewing/climbing). All animal procedures used during the study were reviewed and approved by the Institutional Animal Care and Use Committee at the National Institute for Occupational Safety and Health.

Time-course study design: in vivo lung injury, inflammation and disease

On day 0, rats were lightly anesthetized with an intraperitoneal injection of 30–40 mg/kg sodium methohexital (Brevital; Eli Lilly, Indianapolis, IN) and intratracheally instilled with 7.89 μg DPM, 50 μg DPM, 50 μg SIL, 233 μg SIL, 7.89 μg DPM +233 μg SIL, 50 μg DPM +233 μg SIL, 50 μg DPM +50 μg SIL or vehicle control (PBS). All particles were delivered in 0.3 mL USP-grade PBS. All animals were humanely euthanized at one day, one week, one month or three months following particle exposure ($n = 8$/group/time point) with an intraperitoneal injection of 100–300 mg/kg sodium pentobarbital followed by exsanguination. Additionally, a two-month postexposure time point was incorporated for select dose combinations based on various parameters of toxicity observed in the groups at the one- and three-month time points. The trachea was cannulated, bronchoalveolar lavage (BAL) was performed on the right lung lobes, and BAL cells (BALC) and fluid (BALF) were retained for the analysis of parameters indicative of inflammation, injury, oxidant production and immune function. Lung injury and inflammation were evaluated as the presence of lactate dehydrogenase (LDH) activity, cytokines and chemokines in BALF. BALC were centrifuged onto slides, stained and counted to determine cell phenotype differential. BAL lymphocytes were further differentiated by phenotype by flow cytometry. Lymphocytes from lymph nodes draining the lung were also differentiated by phenotype. Chemiluminescence assays were used to measure oxidant/free radical production by BAL phagocytes to evaluate the inflammatory response. The left lung was excised, pressure-inflated with 10% neutral-buffered formalin and weighed with water displacement to determine fixed lung volume. Histopathological assessment of lung injury, inflammation and disease were performed and morphometric analysis of fibrillar collagen content was conducted.

Infection study design: pulmonary immune response to infection following particle exposure

In this study, rats were exposed to 50 μg DPM, 233 μg SIL, 50 μg DPM +233 μg SIL combined in 0.3 mL PBS or PBS alone (vehicle control) by intratracheal instillation as described above. One week following particle exposure, rats were intratracheally instilled with 5×10^5 colony forming units (cfu) of *Listeria monocytogenes* (strain 10403 S, serotype 1) in 0.5 mL of sterile PBS. Animals were euthanized at 1, 3, 5, 7 and 14 days following infection ($n = 8$/dose/time point). BAL was performed on the right lung lobes, and BALC and BALF were retained for the analysis of parameters indicative of inflammation, injury and immune alteration as described for the time-course study. The left lung was clamped during lavage and subsequently excised, homogenized and cultured to evaluate bacterial clearance from the lung.

BAL

BAL was performed at each time point after exposure. Following euthanasia as described above, the trachea was cannulated, the chest cavity was opened, the left lung bronchus was clamped off, and BAL was performed on the right lung lobes. BAL was recovered in two fractions. The first fraction of the BAL was obtained by inflating the right lung with 4 mL of PBS, massaging for 30 s, withdrawing and repeating the process a second time with the same 4 mL of PBS. The second lavage fraction consisted of repeated 6 mL volumes of PBS instilled with massaging of the chest cavity, withdrawal and combination until a 30 mL volume was recovered. For each animal, both fractions of BAL were centrifuged, the cell pellets were combined and resuspended in 1 mL of PBS, and the acellular fluid from the first fraction was retained for further analysis described for BALF below.

Analysis of LDH activity

The level of LDH activity in the BALF of all treatment groups was measured at each time point after exposure to evaluate cytotoxicity as a measure of lung injury. Measurement of LDH activity in the acellular fluid was obtained using a Cobas Mira chemistry analyzer (Roche Diagnostic Systems; Montclair, IN). LDH activity was

quantified by detection of the oxidation of lactate coupled to the reduction of nicotinamide adenine dinucleotide at a spectrophotometric setting of 340 nm.

BALF protein analysis

Cytokines and chemokines involved in inflammatory and immune responses were measured at each time point after exposure in the BALF of rats treated with PBS, DPM, SIL or DPM/SIL combinations, with commercially available enzyme-linked immunosorbent assay (ELISA) kits or by multiplex array. The following cytokines and chemokines were quantified by ELISA: tumor necrosis factor-α (TNF-α), transforming growth factor-β (TGF-β), interleukin (IL)-10, IL-12p70, monocyte chemotactic protein (MCP)-1, macrophage inflammatory protein (MIP)-2 (Novex, Life Technologies; Grand Island, NY); IL-2, IL-4, IL-6, interferon (IFN)-γ (R&D Systems; Minneapolis, MN); and osteopontin (OPN, Enzo Life Sciences; Farmingdale, NY). Additionally, two matrix metalloproteinases (MMP), MMP-2 and MMP-9, were quantified by ELISA, as well as tissue inhibitor of metalloproteinases (TIMP)-1 (R&D Systems) as indices of tissue remodeling due to injury. IL-1α, IL-1β, IL-5, IL-13, IL-17 A, IL-18, granulocyte colony-stimulating factor (G-CSF), granulocyte and macrophage colony-stimulating factor (GM-CSF), eotaxin, leptin, MIP-1α, epidermal growth factor (EGF), IFN-γ-inducible protein (IP)-10, growth-regulated oncogene/keratinocyte chemoattractant (GRO/KC), vascular endothelial growth factor (VEGF), fractalkine, lipopolysaccharide (LPS)-induced CXC chemokine (LIX) and regulated on activation, normal T-cell expressed and secreted (RANTES) were assessed by multiplex array (Eve Technologies; Alberta, CA).

BALC differentials

Total BALC collected from rats intratracheally instilled with PBS, DPM, SIL or DPM + SIL in combination were counted using a Coulter Multisizer II (Coulter Electronics; Hialeah, FL). BALC differentials were performed to determine the total number of alveolar macrophages (AMs), neutrophils, lymphocytes and eosinophils. Briefly, 5×10^4 cells from each rat were spun down onto slides with a Cytospin 3 centrifuge (Shandon Life Sciences International; Cheshire, England) and labeled with Hema 3® stain (Fisher Scientific; Kalamazoo, MI) to differentiate cell types. Two hundred cells per slide were counted, and the percentage of AMs, neutrophils, lymphocytes and eosinophils was multiplied by the total number of cells to calculate the total number of each cell type.

Chemiluminescence (CL)

To measure the production of reactive oxidant species by BALC, CL was measured according to the method of Antonini et al. (Antonini et al., 1994). Luminol (Sigma-Aldrich; St. Louis, MO) was used as an amplifier to enhance detection of the light, and 0.2 mg/mL of unopsonized zymosan (Sigma-Aldrich) or 3 μM phorbol myristate acetate (PMA; Sigma-Aldrich) was added to the assay immediately prior to the measurement of CL to activate the cells. Because rat neutrophils do not respond to unopsonized zymosan, the zymosan-stimulated CL produced is from AMs, whereas the soluble stimulant, PMA, activates both neutrophils and AMs to generate reactive oxidant species (Castranova et al., 1990). CL was quantified using an automated Berthold Autolumat LB 953 luminometer (Wallace, Inc.; Gaithersburg, MD). Each sample was measured for 15 min, and the integral of counts per minute (cpm) versus time was calculated. The production of CL was calculated as the cpm of stimulated cells minus the cpm of the corresponding resting cells, then normalized to the total number of BAL AMs for zymosan-stimulated CL and total BALC for PMA-stimulated CL.

Phenotypic quantification of BALC and mediastinal lymph node (MLN) cells by flow cytometry

Lymphocyte populations in BALC and MLN were differentially assessed for phenotype by multicolor flow cytometry analysis. Briefly, cells were obtained by BAL or by homogenizing the MLN manually between frosted glass slides followed by filtration. 10^6 cells were plated in a 96-well round bottom plate. Cells were washed and blocked for nonspecific staining using mouse anti-rat CD32 (FCγRII) antibody (BD Pharmingen™; San Diego, CA). Cells were then fluorescently-labeled with one or a combination of the following mouse-anti-rat antibodies to determine phenotype: CD3 (T cells), CD3 and CD4 (T-helper cells), CD3 and CD8a (cytotoxic T cells), CD161a (NKR-P1A; natural killer cells), or CD45R (B220; B Cells) (BD Pharmingen™). Cells were then washed and fixed with BD Cytofix/Cytoperm™ (BD Pharmingen™) and stored at 4 °C until phenotyped using a BD™ LSRII flow cytometer and BD FACSDiva™ software v6 (Becton, Dickinson and Company; San Jose, CA) (within 24 h). Results were gated and analyzed using ©FlowJo Software v10 (FlowJo, LLC; Ashland, OR).

Histopathology

The left lungs of rats were fixed with 10% neutral buffered formalin by airway pressure fixation under 30 cm water pressure to total lung capacity for 15 min. Lung volumes were assessed by weight of water displacement. The left lungs were embedded in paraffin, sectioned onto slides, and stained with hematoxylin and eosin (H&E) or trichrome. An $n = 5$ stained slides for DPM 7.89 μg, DPM 50 μg, DPM 7.89 μg in combination with SIL 233 μg and DPM 50 μg in combination with SIL 233 μg were evaluated for each time point of one week, one month and three months. Additionally, saline, DPM 50 μg, SIL 233 μg and DPM 50 μg in combination with SIL 233 μg were also evaluated for the 2-month time point. Study blocks were designed with paired controls resulting in $n = 10$ stained slides evaluated for saline and SIL 233 μg groups (five from each of the study blocks when combined) for one week, one month

and three- month time points. Stained slides were analyzed for indications of inflammation, injury and fibrosis by a certified veterinary pathologist at Charles River Laboratories (Wilmington, MA) who was blinded to the treatment groups. Indices of pathology were scored on scale of 0–5, where 0 = no observed effect, 1 = minimal response, 2 = mild response, 3 = moderate response, 4 = marked response and 5 = severe response.

Morphometric analysis of connective tissue thickness

Tissue sections from left lung were deparaffinized and stained with Sirius Red for detection of connective tissue, particularly fibrillar collagen. Slides were immersed in 0.1% picrosirius solution (100 mg of Sirius Red F3BA in 100 ml of saturated aqueous picric acid) for 2 h followed by washing for 1 min in 0.01 N HCl. Slides were then counterstained with hematoxylin for 2 min, dehydrated and mounted with a coverslip for imaging. Quantitative morphometric methods were used to measure the average thickness of Sirius Red-positive connective tissue in the alveolar regions. Volume (% of the alveolar wall) and thickness were measured by standard morphometric analyzes that consisted of basic point and intercept counting (Mercer et al., 1994; Underwood, 1970). Grid pattern, X and Y boundaries and number of intersections were determined as previously described (Roberts et al., 2012). Volume was determined by counting the number of points over the Sirius Red-positive connective tissues in the alveolar regions. Surface density of the alveolar wall was determined from intercepts between a line overlay and the alveolar wall. To limit the measurements to alveolar parenchyma, areas containing airways or blood vessels 25 µm in diameter were excluded from the analysis. Average thickness of the Sirius Red-positive connective tissue of the alveolar wall was computed as from two times the ratio of volume density of point to the surface density of the alveolar wall.

Bacterial clearance from the lung

To measure the clearance of bacteria from the lung, left lungs were excised and placed in 10 mL of sterile deionized water. Lungs were homogenized using a Polytron®PT-2100 homogenizer with PT-DA 2112/EC aggregate attachment (Kinematica; Bohemia, NY). Homogenates were diluted and cultured on prepared Brain Heart Infusion Agar plates (Becton, Dickinson and Company). Cultures were incubated at 37 °C for 24 h. Cfu were counted and multiplied according to culture dilution factors.

Statistical analyses

Results for all BAL parameters, cellular phenotype, morphometry and bacterial clearance were expressed as mean fold change from control calculated as $\frac{\bar{x}}{control\,\bar{x}}$ and a one way analysis of variance (ANOVA) was performed between all treatments groups at each time point. Significant differences among groups were determined using the Student–Newman–Keuls *post hoc* test. Data were analyzed using SigmaPlot for Windows Version 12.5 (Systat Software, Inc.; Ekrath, Germany). For all analyses, significance was set at $p < .05$. Because data from histopathology studies are inherently categorical, nonparametric analysis of variance was assessed using SAS/STAT software, Version 9.1, of the SAS System for Windows statistical programs (SAS Institute, Inc.; Cary, NC). In this instance, groups were compared using the Wilcoxon rank sum test.

Results

Particle characterization

One ml aliquots of 7.89 µg dose DPM, 50 µg dose DPM, 233 µg dose of SIL, as well as 7.89 µg and 50 µg DPM in combination with SIL 233 µg (DS) in PBS solution, were dried on carbon filters and examined using FESEM in order to characterize size of the primary particles and their degree of agglomeration. In solution, DPM was found to agglomerate to a size of approximately 2 µm in diameter. The primary particle size was found to be smaller in size, ~200 nm. The primary particles of SIL were approximately 2 µm in size and were evenly distributed in suspension (Figure 1(A,B)). The association between DPM and SIL in solution was minimal. EDX was used to evaluate the elemental components of each particle. DPM was found to be composed of primarily carbon, reflecting the carbonaceous core of the DPM, with very little detectable trace elements including: chromium, copper, iron, nickel, oxygen, silicon and zinc adsorbed to it (Figure 1(C)). The EDX spectrum of the SIL sample is depicted in Figure 1(D).

Time-course study

Lung injury was evaluated by examining LDH in the BALF collected from rats at one day, one week, one month, two months and three months postexposure to particles. LDH activity was significantly increased in all groups that contained the high dose of SIL (233 µg) and the high dose of SIL alone at all time points following exposure when compared to control (Figure 2). At early time points, the increase in groups that were coexposed to SIL and DPM was primarily driven by SIL particles. However, by 3 months, coexposure to the high doses of DPM and SIL (DS 50/233) resulted in an increase when compared to all other groups. There were no significant increases in LDH activity in groups exposed to DPM alone at either dose, SIL 50 alone, or DS 50/50.

Protein mediators were evaluated in BALF as a measure of inflammation and immune response (Table 1). The low dose of DPM (DPM 7.89) and the low dose of silica (SIL 50) did not cause any significant changes in BALF protein when compared to control with the exception of DPM 7.89, whereby IL-10 was significantly elevated (data not shown). The high dose of SIL caused increases in several proteins associated with inflammation; MCP-1, MIP-1α, RANTES, GRO/KC, MIP-2, IP-10, TNF-α and IFN-γ compared with the control and groups exposed to DPM only. SIL 233 alone

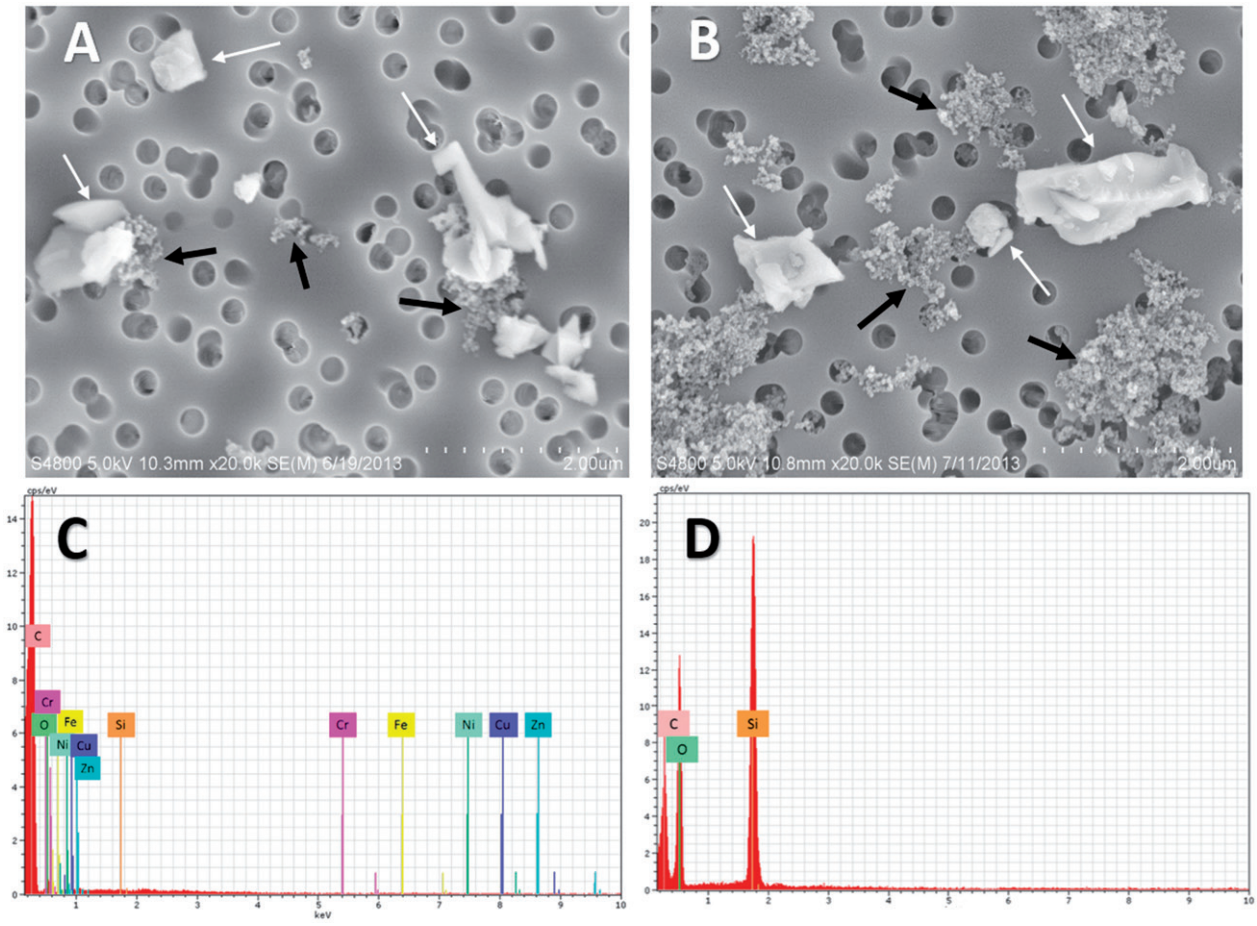

Figure 1. FESEM images of particles. (A) 233 μg SIL and 7.89 μg DPM in combination prepared in PBS solution, diluted 1:10 in PBS, then dried onto a filter under 20,000x magnification (scale bar = 2 μm with 10 segments of 0.2 μm each) (B) 233 μg SIL and 50 μg DPM prepared in PBS solution, diluted 1:10 in PBS, then dried onto a filter in PBS solution under 20,000x magnification (scale bar = 2 μm with 10 segments of 0.2 μm each). White arrows indicate SIL and black arrows indicate DPM. (C) EDX of DPM particles pictured in the FESEM above at 20 keV. Labeled spectral peaks for elements primarily present in the samples. All peaks besides carbon are elements commonly found in DPM but present only in trace amounts in this sample (chromium, copper, iron, nickel, oxygen, silicon and zinc). (D) EDX of SIL particles pictured in FESEM above at 20 keV.

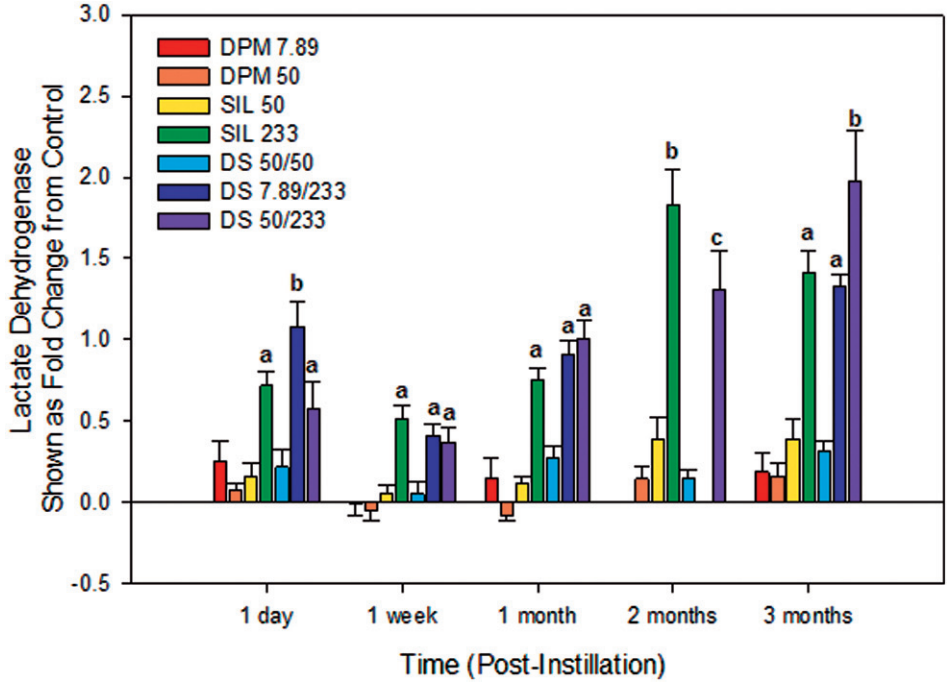

Figure 2. LDH activity in BALF after exposure to DPM, SIL or a combination of DPM and SIL (DS) at indicated doses (μg). Data are shown as mean fold change over control ($y = 0$). Neither DPM 7.89 μg nor DS 7.89/233 μg were evaluated at 2 months. [a]Different from control, DPM 7.89 μg, DPM 50 μg, SIL 50 μg, DS 50/50 μg groups; [b]different from all other groups; [c]different from control, DPM 50 μg, SIL 50 μg and DS 50/50 μg groups. Statistical significance is $p \leq .05$.

Table 1. Immunoregulatory proteins recovered from BALF of Sprague-Dawley Rats exposed to DPM, SIL or combination of DPM and SIL.

	Group & Dose (μg)	MCP-1	MIP-1α	RANTES	GRO/KC	MIP-2	IP-10	TNF-α	IFN-γ	IL-2	IL-10	OPN	MMP-2	MMP-9	IL-18
Day-1 postexposure	DPM 50	0.95 ± 0.36	1.02 ± 0.93	−0.21 ± 0.12	1.27 ± 1.34	0.70 ± 0.45	3.05 ± 1.03	0.19 ± 0.21	−0.96 ± 0.04	BLD	0.78 ± 0.41	−0.19 ± 0.12	0.63 ± 0.14	0.60 ± 0.89	0.14 ± 0.05
	SIL 233	2.11 ± 0.69	2.37 ± 0.73	0.13 ± 0.23	4.59 ± 0.65^{+}	1.16 ± 0.15	4.01 ± 0.97$^{@}$	1.64 ± 0.47	1.41 ± 0.94$^{\wedge}$	2.18 ± 2.97	0.34 ± 0.30	0.55 ± 0.28	1.56 ± 0.38*	3.72 ± 0.53*	0.41 ± 0.15
	DS 50/233	1.29 ± 0.65	0.98 ± 0.43	−0.08 ± 0.15	0.81 ± 0.89	0.52 ± 0.29	3.09 ± 1.32	1.56 ± 0.57*	−0.85 ± 0.07	BLD	0.04 ± 0.30	0.89 ± 0.35*	0.89 ± 0.19	2.86 ± 0.52*	0.24 ± 0.12
Week-1 postexposure	DPM 50	−0.71 ± 0.16	−0.27 ± 0.05	0.07 ± 0.22	−0.32 ± 0.07	0.24 ± 0.19	1.02 ± 0.79	−0.26 ± 0.11	BLD	BLD	−0.10 ± 0.34	−0.14 ± 0.08	0.10 ± 0.19	1.38 ± 0.80	−0.22 ± 0.11
	SIL 233	1.31 ± 0.50	3.54 ± 0.95^{+}	1.12 ± 0.22	3.76 ± 0.24^{+}	0.68 ± 0.19	4.05 ± 1.20	0.42 ± 0.19*	−0.50 ± 0.22	1.43 ± 1.56	−0.95 ± 0.03*	0.01 ± 0.06	−0.05 ± 0.12	29.25 ± 5.36^{+}	0.32 ± 0.08$^{\&}$
	DS 50/233	1.35 ± 1.11	1.13 ± 0.19	0.57 ± 0.48	1.32 ± 0.61*	0.31 ± 0.08	3.15 ± 1.42	0.34 ± 0.06*	BLD	BLD	−0.83 ± 0.09*	0.19 ± 0.20	−0.08 ± 0.12	14.55 ± 2.05*	0.29 ± 0.10*
Month-1 postexposure	DPM 50	−0.38 ± 0.28	−0.04 ± 0.06	0.11 ± 0.12	−0.43 ± 0.08	−0.02 ± 0.08	−0.59 ± 0.09	−0.07 ± 0.11	BLD$^{@}$	BLD	−0.44 ± 0.15	−0.11 ± 0.06	−0.09 ± 0.11	0.09 ± 0.43	−0.62 ± 0.02
	SIL 233	26.06 ± 7.70*	4.73 ± 0.98*	1.33 ± 0.15*	2.32 ± 0.22*	0.41 ± 0.10*	1.88 ± 0.87	0.48 ± 0.35	−0.37 ± 0.27	1.65 ± 1.77	−0.49 ± 0.16	0.63 ± 0.21*	0.50 ± 0.15*	17.67 ± 5.72*	−0.20 ± 0.09
	DS 50/233	43.41 ± 9.70*	3.94 ± 1.06*	1.19 ± 0.26*	1.96 ± 0.15*	0.16 ± 0.10	3.31 ± 1.80	0.50 ± 0.31	−0.96 ± 0.04$^{@}$	BLD	−0.82 ± 0.10$^{@}$	1.03 ± 0.25*	0.61 ± 0.15*	24.20 ± 4.85*	−0.35 ± 0.09
Month-2 postexposure	DPM 50	0.17 ± 0.59	0.09 ± 0.25	0.33 ± 0.31	−0.66 ± 0.12	0.09 ± 0.08	0.06 ± 0.21	−0.28 ± 0.17	0.36 ± 0.52	0.29 ± 0.51	0.09 ± 0.08	−0.21 ± 0.17	0.71 ± 0.34	0.87 ± 0.76	0.17 ± 0.24
	SIL 233	23.26 ± 3.92*	5.42 ± 0.95*	0.03 ± 0.18	−0.28 ± 0.19	0.10 ± 0.03	1.85 ± 0.49*	0.36 ± 0.10$^{\&}$	1.01 ± 0.64	−0.11 ± 0.38	±0.36 ± 0.03*	8.09 ± 1.78^{+}	0.39 ± 0.18	5.98 ± 1.74*	1.43 ± 0.28^{+}
	DS 50/233	19.90 ± 5.76*	4.93 ± 0.93*	−0.19 ± 0.13	−0.27 ± 0.23	−0.09 ± 0.07	2.21 ± 0.75*	0.34 ± 0.12$^{\&}$	0.44 ± 0.47	0.90 ± 0.83	−0.41 ± 0.04*	3.49 ± 1.34$^{@}$	0.12 ± 0.10	4.37 ± 0.55$^{@}$	0.81 ± 0.22$^{@}$
Month-3 postexposure	DPM 50	−0.20 ± 0.36	0.31 ± 0.17	0.15 ± 0.16	−0.21 ± 0.19	0.05 ± 0.09	−0.12 ± 0.21	0.28 ± 0.38	BLD	BLD	−0.20 ± 0.08	−0.27 ± 0.07	−0.12 ± 0.11	0.52 ± 0.38	0.10 ± 0.11
	SIL 233	20.37 ± 5.62*	7.62 ± 1.59*	0.90 ± 0.11*	2.66 ± 0.35*	0.25 ± 0.17	4.83 ± 1.28*	1.05 ± 0.15$^{@}$	1.12 ± 0.89	−0.56 ± 0.22	−0.40 ± 0.10	1.08 ± 0.27*	−0.44 ± 0.09	62.17 ± 23.11*	1.31 ± 0.35*
	DS 50/233	23.34 ± 8.34*	9.51 ± 3.05*	1.08 ± 0.25*	2.15 ± 0.71*	0.15 ± 0.08	3.51 ± 1.25*	0.98 ± 0.17*	−0.65 ± 0.21	−0.96 ± 0.03	−0.44 ± 0.14	0.98 ± 0.42*	−0.13 ± 0.08	87.60 ± 21.95*	1.47 ± 0.22*

All data are shown as mean fold change over control ± standard error.
*Different from control and DPM 50 μg.
^Different from DPM 50 μg and DS 50/233 μg groups.
$^{+}$Different from all other groups.
$^{\&}$Different from DPM 50 μg.
$^{@}$Different from control.
Results that were below the limit of detection (BLD) were noted.
Half of the lowest limit of detection was used for statistical analysis of values BLD. Statistical significance is $p \leq .05$.

and the DS 50/233 groups caused a decrease in the anti-inflammatory protein IL-10 from one week to 2 months postexposure compared with control and DPM-exposed groups. SIL 233 alone and the DS 50/233 groups also caused a significant increase in MMP-9, a protein associated with tissue remodeling which has implications in the development of fibrotic changes in the lung, at all time points following exposure. Additionally, SIL high-dose exposure increased MMP-2 and OPN, additional proteins associated with tissue remodeling, wound healing and fibrosis at one month post exposure and at all time points thereafter for OPN. Finally, the SIL high dose alone or in combination with the DPM high dose caused an increase in IL-18, a protein associated with upregulation of the NLRP3/NALP3 inflammasome, at later time points. DPM 50 alone did not illicit an increase in pro-inflammatory cytokines. However, the high dose of DPM did cause a decrease in IL-2 and IFN-γ proteins associated with the effector properties of T_h1 cells, when compared with controls. The decrease in IL-2 was also present in the high-dose coexposure group (DS 50/233). Similarly, DPM in combination with SIL exhibited independent action on the expression of some cytokines like, MIP-α, GRO/KC, MIP-2, MMP-2 and MMP-9 at some time points (Table 1), suggesting that DPM in a coexposure may have the capability to reduce the effects observed with SIL alone. These observations may indicate altered macrophage and lymphocyte activity in response to treatment with DPM. There were no significant changes in the following cytokines in any group: EGF, eotaxin, fractalkine, G-CSF, GM-CSF, IL-1α, IL-1β, IL-4, IL-5, IL-6, IL-12p70, IL-13, IL-17 A, leptin, LIX, TGF-β, TIMP-1 and VEGF (data not shown).

Cell differentials were performed on BALC to further assess inflammation (Figure 3(A,B)). DPM alone at either dose did not cause an increase in the influx of AMs (Figure 3(A)) or neutrophils (Figure 3(B)). AM influx was increased in all groups that contained SIL 233 beginning at one-week postexposure. Neutrophil influx significantly increased as early as one-day postexposure in all groups containing SIL 233 (Figure 3(B)) and persisted throughout the time course. Exposure to SIL 50 μg showed a trend toward an increase in neutrophils up to one month following exposure with resolution of response over time. At one month, exposure to DS 50/233 caused a significant increase in neutrophils when compared to all groups. The DS50/50 group followed a similar pattern as SIL 50 alone. BALC activation was also evaluated as oxidant production *ex vivo* (Figure 3(C,D)). DPM only doses used in this study did not cause an increase in oxidant production by AMs and neutrophils as measured by CL. Oxidant production in the SIL 233 group significantly increased for both total phagocytes at one day and at three months postexposure (Figure 3(C)) and oxidant production by macrophages followed a similar pattern (Figure 3(D)). Interestingly, exposure to the higher dose of DPM combined with the high dose of SIL resulted in significantly increased oxidant production over exposure to the high dose of SIL alone at one week, one month and two months postexposure, suggesting a higher

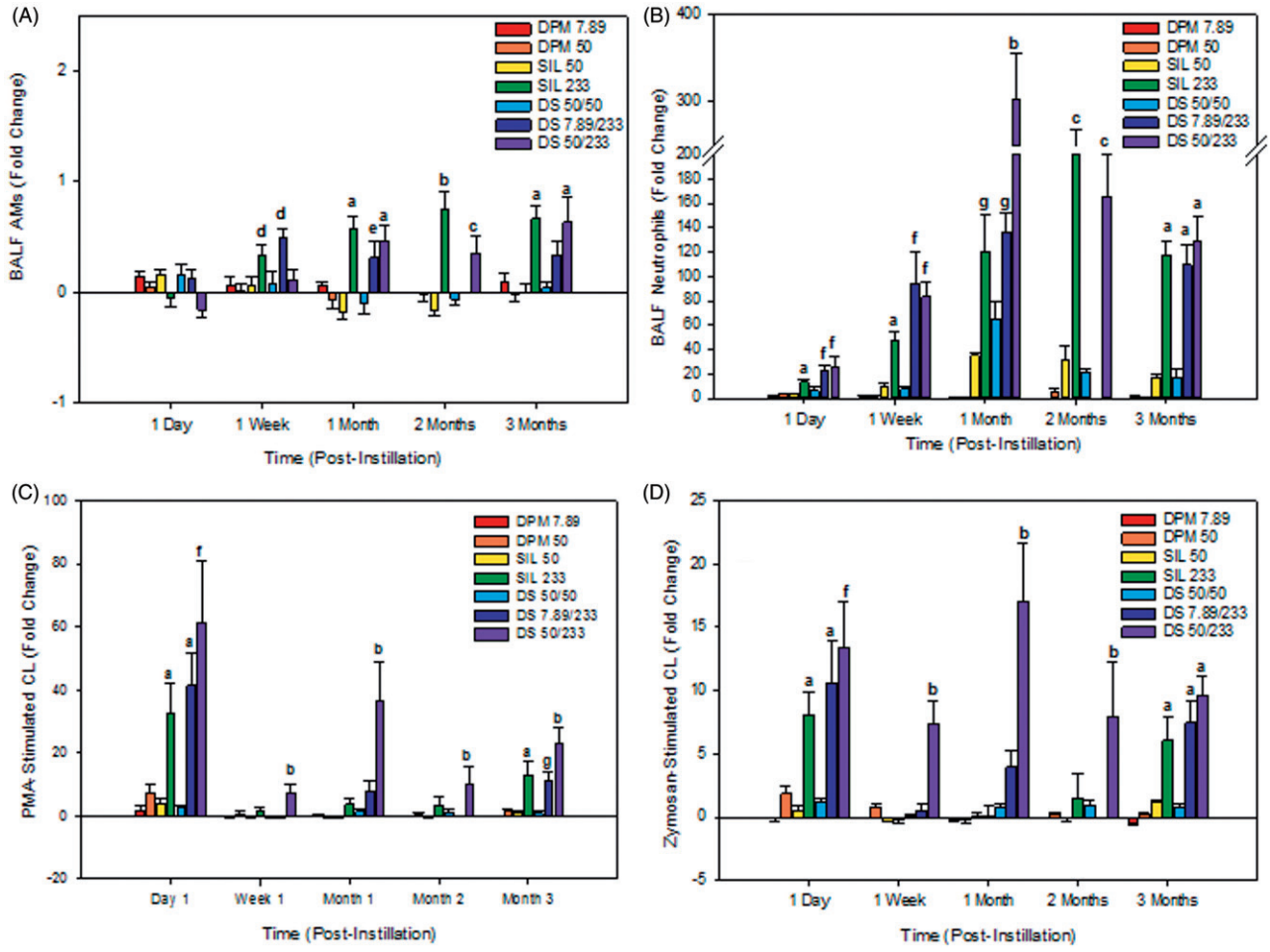

Figure 3. Total AMs (A) and neutrophils (B) in the BALF following exposure to DPM, SIL or DS at doses indicated. Production of oxidants by total phagocytes stimulated with PMA (C) or by AMs only stimulated by zymosan (D) measured by chemiluminescence following exposure to DPM, SIL or DS at doses indicated. DPM 7.89 μg was not evaluated at 2 months. All data are shown as a mean fold change over control ($y = 0$). [a]Different from control, DPM 7.89 μg, DPM 50 μg, SIL 50 μg, DS 50/50 μg groups; [b]different from all other groups; [c]different from control, DPM 50 μg, SIL 50 μg, and DS 50/50 μg groups; [d]different from control and DPM 50 μg only; [e]different from control, DPM 50 μg, and SIL 50 μg groups; [f]different from control, DPM 7.89 μg, DPM 50 μg, SIL 50 μg, SIL 233, and DS 50/50 μg; [g]different from control, DPM 7.89 μg, DPM 50 μg and SIL 50 μg groups. Statistical significance measured as $p \leq .05$.

oxidant burden in the lung of rats in the high-dose coexposure group at these times.

BAL and MLN lymphocytes were phenotyped by flow cytometry. In addition to phagocytic influx described in Figure 3, exposure to SIL at the high dose alone or in combinations with DPM 50 caused significantly increased lymphocyte influx into the lung as early as one day following exposure (Table 2) and proliferation in the MLN as early as one-week postexposure (Table 3). This effect was attributed primarily to $CD4^+$ and $CD8^+$ T-cell population subsets. Exposure to DPM 50 alone did not cause a significant increase in lymphocyte populations in BAL or MLN. Additionally, it was noted that for the coexposed group, DPM exhibited independent action reducing the influx of the $CD8^+$ subset of cells into the lung observed with the SIL only exposed group at one month and total T cells, which was mostly attributed to reduced influx of the $CD4^+$ T cell subset, at three months following exposure.

H&E and trichrome-stained tissue sections were evaluated by a board certified veterinarian pathologist (Table 4). DPM alone at either dose did not cause pathological changes in the lung. Influx of AMs, as a measure of inflammation, was significantly elevated in the SIL 233 group alone at all time points following exposure and when combined with DPM at one month following exposure. Alveolar epithelial hyperplasia (AEH) was also observed at all points following exposure in DS 50/233-exposed groups. At one month following exposure to particles, minimal to mild septal fibrosis was observed in groups exposed to SIL 233. Interestingly, incidence of septal fibrosis was significantly increased by coexposure to the high doses of DPM and SIL at one month. By three months after exposure, occurrence of septal fibrosis was equivalent in both SIL 233 only and coexposed groups. Groups exposed to SIL in combination with high-dose DPM scored significantly higher for particles in tissue versus DPM alone as indicated by the presence of brown granules accumulated in macrophages, which corresponds to an observation of increased coloration in lymph nodes as well. Furthermore, mild hyperplasia of the bronchiolar/alveolar epithelium was observed near the terminal bronchioles at two months following exposure and was found to be associated with the presence of macrophages loaded with high particle content, suggesting a correlation between tissue damage and the presence of particles (data not shown). SIL

Table 2. Lymphocyte phenotype determination by flow cytometry in the BALF recovered from Sprague-Dawley rats exposed to DPM, SIL or DPM and SIL combined.

	Exposure (μg)	Total lymphocytes	T cells	$CD4^+$ T cells	$CD8^+$ T cells	B cells
Day-1 postexposure	DPM 50	0.34 ± 0.20	0.27 ± 0.36	0.97 ± 0.77	0.42 ± 0.18	0.11 ± 0.24
	SIL 233	1.81 ± 0.44*	0.90 ± 0.41	1.41 ± 0.74	1.71 ± 0.94	0.66 ± 0.35
	DS 50/233	1.49 ± 0.48*	0.68 ± 0.39	2.02 ± 0.76	0.34 ± 0.21	0.47 ± 0.23
Week-1 postexposure	DPM 50	−0.05 ± 0.16	0.22 ± 0.19	0.63 ± 0.26	0.17 ± 0.21	0.36 ± 0.34
	SIL 233	4.25 ± 0.91*	2.29 ± 0.51*	8.73 ± 2.19*	5.28 ± 1.18*	0.30 ± 0.17
	DS 50/233	2.68 ± 0.61*	3.30 ± 0.80*	13.75 ± 3.63*	5.51 ± 0.57*	0.17 ± 0.20
Month-1 postexposure	DPM 50	−0.11 ± 0.17	−0.16 ± 0.21	−0.14 ± 0.14	0.37 ± 0.24	−0.09 ± 0.37
	SIL 233	3.57 ± 0.95*	2.45 ± 0.83*	8.08 ± 2.59*	10.52 ± 5.12*	0.82 ± 0.44
	DS 50/233	3.34 ± 0.59*	2.54 ± 0.51*	10.06 ± 2.11*	6.80 ± 1.73&	0.49 ± 0.15
Month-2 postexposure	DPM 50	−0.05 ± 0.11	0.80 ± 0.51	1.16 ± 0.66	0.51 ± 0.46	0.56 ± 0.39
	SIL 233	1.67 ± 0.21*	3.98 ± 0.69*	5.63 ± 0.92*	3.00 ± 0.90*	2.30 ± 0.51*
	DS 50/233	1.30 ± 0.35*	3.19 ± 0.86*	4.91 ± 1.22*	1.74 ± 0.59	1.37 ± 0.83
Month-3 postexposure	DPM 50	0.01 ± 0.09	0.11 ± 0.15	0.31 ± 0.39	−0.20 ± 0.15	−0.11 ± 0.13
	SIL 233	3.35 ± 0.27*	4.22 ± 1.05+	12.26 ± 3.33+	2.70 ± 0.74*	0.56 ± 0.23
	DS 50/233	3.18 ± 0.88*	2.25 ± 0.45*	5.29 ± 0.84*	3.24 ± 0.57*	0.21 ± 0.19

All data are expressed as mean fold change over control ± standard error.
*Different from control and DPM 50 μg.
&Different from DPM 50 μg.
+Different from all other groups.
Statistical significance is $p \leq .05$.

Table 3. Lymphocyte phenotype determination by flow cytometry in the MLN excised from Sprague-Dawley rats exposed to DPM, SIL or DPM and SIL combined.

	Exposure (μg)	Total lymphocytes	T cells	$CD4^+$ T cells	$CD8^+$ T cells	B cells
Day-1 postexposure	DPM 50	0.09 ± 0.12	0.18 ± 0.15	0.17 ± 0.14	0.26 ± 0.18	−0.01 ± 0.09
	SIL 233	0.24 ± 0.12	0.24 ± 0.12	0.17 ± 0.12	0.35 ± 0.15	0.22 ± 0.11
	DS 50/233	0.48 ± 0.20	0.53 ± 0.25	0.45 ± 0.23	0.76 ± 0.32	0.43 ± 0.18
Week-1 postexposure	DPM 50	0.35 ± 0.14	0.39 ± 0.17	0.44 ± 0.19	0.36 ± 0.17	0.29 ± 0.13
	SIL 233	1.24 ± 0.10*	1.50 ± 0.11*	1.44 ± 0.12*	1.73 ± 0.24*	0.99 ± 0.11*
	DS 50/233	1.37 ± 0.23*	1.56 ± 0.23*	1.53 ± 0.23*	1.58 ± 0.28*	0.99 ± 0.21*
Month-1 postexposure	DPM 50	−0.05 ± 0.08	0.01 ± 0.08	0.04 ± 0.09	−0.04 ± 0.09	−0.10 ± 0.09
	SIL 233	0.70 ± 0.24*	1.00 ± 0.31*	0.94 ± 0.31*	1.19 ± 0.34*	0.53 ± 0.19*
	DS 50/233	0.87 ± 0.15*	1.36 ± 0.25*	1.17 ± 0.26*	1.71 ± 0.32*	0.60 ± 0.11*
Month-2 postexposure	DPM 50	0.02 ± 0.12	0.10 ± 0.13	0.18 ± 0.12	0.003 ± 0.15	0.03 ± 0.12
	SIL 233	2.91 ± 0.43*	3.79 ± 0.59*	3.76 ± 0.66*	4.07 ± 0.58*	2.98 ± 0.43*
	DS 50/233	3.23 ± 0.26*	3.89 ± 0.33*	3.66 ± 0.33*	4.62 ± 0.48*	3.52 ± 0.41*
Month-3 postexposure	DPM 50	0.11 ± 0.04	0.02 ± 0.06	0.09 ± 0.07	−0.14 ± 0.12	0.15 ± 0.05
	SIL 233	4.98 ± 1.17*	6.02 ± 1.38*	5.17 ± 1.11*	7.97 ± 1.89*	4.46 ± 1.15*
	DS 50/233	4.74 ± 0.70*	5.92 ± 0.90*	5.30 ± 0.71*	6.84 ± 1.41*	4.34 ± 0.71*

All data are shown as mean fold change over control ± standard error.
*Different from control and DPM 50 μg.
Statistical significance is $p \leq .05$.

50 and DS 50/50 were not evaluated as BAL parameters of injury and inflammation were not increased in the DS50/50 coexposure group. Overall, most histopathological changes were attributable to exposure to 233 μg of SIL; however, the presence of DPM often increased the severity and/or incidence of these changes in the coexposure groups.

To further quantify observations of fibrosis, alveolar expansion, alveolar septal wall thickness and thickness of fibrillar collagen were measured by morphometry to further assess the fibrotic response to exposure. Alveolar expansion was measured as a ratio of the total airspace volume to volume versus the surface to volume of the epithelial surface intercepts or thickness of airspace between alveolar tissues. Alveolar septal wall thickness was measured as a ratio of the total volume to volume of alveolar tissue versus the surface to volume of epithelial surface intercepts. No significant differences were observed between the treatment groups. Additionally, fibrillar collagen thickness was measured as the ratio of total collagen volume to volume versus total epithelial surface intercepts surface to volume. This measurement is indicative of fibrotic development in lung tissue. Although not statistically significant, there was a trend for increased fibrillar collagen volume in SIL 233-exposed groups and this trend was further increased for coexposed groups at the latest time points measured (data not shown).

Infection study

In order to investigate the effects of particle exposure on respiratory susceptibility to a bacterial pathogen, an infectivity study was conducted to assess the clearance of *L. monocytogenes* from the lung over a 14-day time course one week following exposure to particles. Despite lung inflammation and phagocytic cell activity observed in the absence of infection in coexposed groups (Figure 3), overall clearance of the pathogen was not significantly altered between these

Table 4. Severity and incidence scores for left lung lobes of Sprague-Dawley rats exposed to DPM, SIL or DPM and SIL combined in varying doses.

Exposure group (μg)	Time postexposure	AM	AEH	BH	LNI	BG	F
Control	1 week	0.2 (2/10) D	0	0.1 (1/10) M	0	0	0
DPM 7.89	1 week	0	0	0	0	0	0
DPM 50	1 week	0.2 (1/5) D	0	0	0	0	0
SIL 233	1 week	1.3 (10/10) D[f]	0	0	0.1 (1/10) M	0	0
DS 7.89/233	1 week	1 (5/5) D	0	0.2 (1/5) M	0	0	0
DS 50/233	1 week	2 (5/5) D[d,*]	0.4 (2/5) M[e]	0	0	0.4 (2/5) M[e]	0
Control	1 month	0.3 (3/10) D	0	0	0	0	0
DPM 7.89	1 month	1 (5/5) D	0	0	0	0	0
DPM 50	1 month	0	0	0	0	0	0
SIL 233	1 month	1.7 (10/10) D[b,*]	0.3 (3/10) M	0	0	0	0.2 (2/10) M
DS 7.89/233	1 month	1.8 (5/5) D[b]	0.4 (2/5) M	0	0	0	0.2 (1/5) M
DS 50/233	1 month	1.8 (5/5) D[b]	1 (5/5) M[d,*]	0	0	0.8 (4/5) M[a,*]	0.8 (4/5) M[d,**]
Control	3 months	0.5 (5/10) D	0	0	0	0	0
DPM 7.89	3 months	0.6 (3/5) D	0	0	0	0	0
DPM 50	3 months	0.8 (4/5) D	0	0	0	0	0
SIL 233	3 months	1.8 (10/10) D[f,**]	1.1 (10/10) M[d,**]	0	0	0	1 (8/10) M[c,*]
DS 7.89/233	3 months	2 (5/5) D[f,**]	1 (5/5) M[c]	0	0	0	1 (5/5) M[c]
DS 50/233	3 months	1.4 (5/5) D	1.4 (5/5) M[d,**]	0	0	0.6 (3/5) M[a,*]	0.8 (3/5) M

Lung tissue was analyzed and scored for accumulation of alveolar macrophages as an index of inflammation (AM), alveolar epithelial hyperplasia (AEH), bronchus associated lymphoid tissue hyperplasia (BH), lymphoid nodules in the interstitium (LNI), brown granules in alveolar macrophages (BG; the presence of DPM particles), fibrosis in alveolar septae (F) ($n = 5$ or 10 per group per time point). Severity was scored as 0–5: 0 = normal, 1 = minimal/slight, 2 = mild, 3 = moderate, 4 = marked and 5 = severe. Incidence was noted as Focal (F), Multi-focal (M), and Diffuse (D). Data are presented as means with incidence (number of animals with a positive score per total animals) in parentheses.
[a]Different from all other groups.
[b]Different from control and DPM 50 μg only.
[c]Different from control only.
[d]Different from control, DPM 7.89 μg, and DPM 50 μg group.
[e]Different from control and SIL 233 μg group.
[f]Different from control and DPM 7.89 μg group.
All notations indicate a p value $<.05$ except where asterisks indicate $^{*}p < .01$ and $^{**}p < .05$ for all groups except control where $p < .01$.

treatment groups (Figure 4(A)). The data suggest that, for the doses of DPM used in this study, which were not found to induce toxicity by themselves, combination with moderately toxic doses of SIL did not alter susceptibility to an infection with *Listeria monocytogenes*. Influx of cells into the lungs was significantly increased for SIL 233–exposed groups at day-1 postinfection (Figure 4). This influx appeared to be comprised mostly of neutrophils (Figure 4(D)) and lymphocytes. By day-3 postinfection, the influx of cells in SIL 233–exposed groups was resolved. Finally, cells from the BAL and MLN were phenotyped as in the time-course study to evaluate lymphocyte populations. For the SIL-233-exposed group, the influx of lymphocytes into the BAL at day-1 postinfection was significantly greater when compared with the control group and again on day 14. DPM exposure caused no significant alterations in lymphocyte influx into the lung, while combined exposure to particles caused significant increases in total lymphocyte influx at day 14 compared with control and DPM exposed groups comprised mostly of $CD4^+$ cells (Table 5). In the MLN, the SIL 233–exposed group had significantly increased lymphocytes, specifically $CD4^+$ T Cells, compared with control and overall T-cell populations were significantly increased when compared to control and DPM 50 at day-1 postinfection. SIL-233 exposure also increased total lymphocytes in the MLN compared with all other groups at day-3 postinfection. DPM exposure caused significant decreases compared with SIL-exposed group for total T cells at day-3 postinfection and caused significant decreases in the $CD8^+$ subset of T cells compared with SIL-233 and control groups for the same time point. Finally, combined exposure caused increased lymphocytes at day 1 for total cells and total T cells compared with control group and compared with DPM and control for the $CD4^+$ T-cell subset (Table 6).

Discussion

The current study was conducted in order to address a knowledge gap with relation to coexposures representative of those which may occur in mining industry occupations, including hydraulic fracturing. It is important to note that the DPM used in this study was extracted from DE collected from an industrial forklift in the 1990s, which qualifies it as "transitional" in nature (collected between 1988 and 2006). Transitional DE samples vary from "traditional" DE or "TDE" (collected prior to 1988) and New Technology DE or "NTDE" (collected post-2006) in chemical and physical properties. TDE is considered to be more hazardous in nature due to having a larger amount of particulate matter, carbon monoxide and hydrocarbon emissions while NTDE has significantly lower TDE-related emissions (Hesterberg et al., 2009); however, very little information is available on health outcomes related to NTDE exposure. Additionally, the current study examined DPM only and not total DE, which contains higher levels of metals and hydrocarbons, which in turn may lead to greater toxicity following exposure to DE. The silica used in this study was also a surrogate for occupational exposures that occur in mining operations and oil and gas extraction. It is not a freshly fractured form of crystalline silica, which has been shown to be higher in toxicity than aged silica (Vallyathan et al., 1995), and although sand used at hydraulic fracturing sites contains

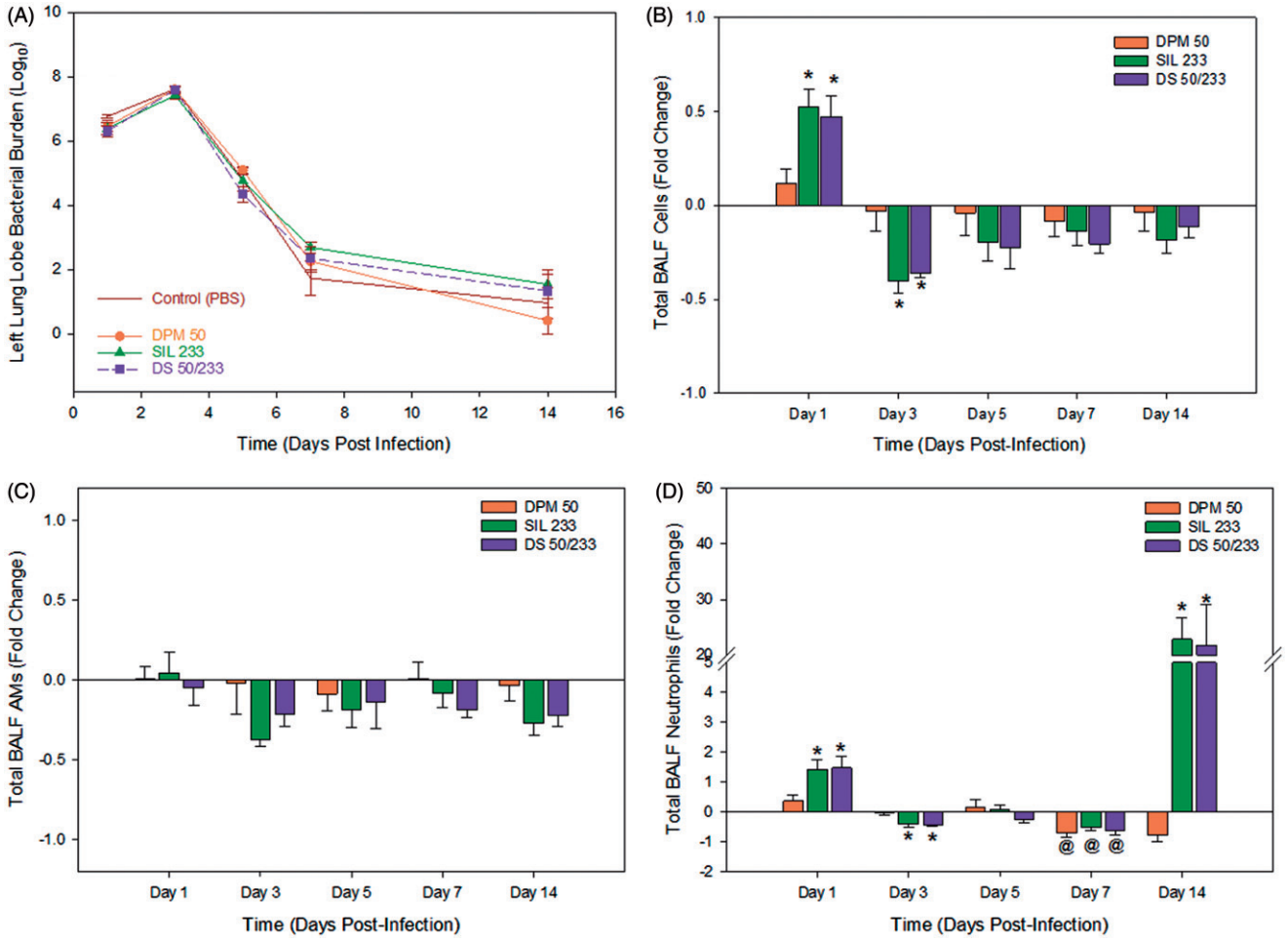

Figure 4. (A) Bacterial burden in the left lung over the time course. Data are shown on a $\log_{10}$ scale. Total cells (B), total AMs (C) and total neutrophils (D) recovered by lavage following exposure to DPM, SIL or DS at doses indicated. (B–D) Data are shown as a mean fold change over control ($y = 0$). *Different from control and DPM 50 μg; @different from control. Statistical significance is $p \leq .05$.

respirable silica, composition of the sand may vary from site to site (Beckwith, 2011; Brown, 2012).

While most parameters of toxicity evaluated could be attributed to the more reactive and toxic crystalline silica particles, DPM, at doses that represent different durations of exposure based on field measures taken at mining sites and OELs, did exacerbate the effects of silica in the acute exposure model examined, particularly between 1 week and 1 month post-exposure. This exacerbation was observed for the parameters of pulmonary inflammation, quantified by the influx of neutrophils into the lung (Figure 3(B)) as well as by the oxidant production by phagocytes (Figure 3(C,D)) at time points up to one month for inflammation and up to three months for oxidant production. Furthermore, assessment of pathology in the lung tissue suggested that DPM may be contributing to the mild fibrotic response induced by silica in the lung, whereby there was an increased incidence of mild fibrosis at one-month postexposure in the animals that were exposed to the combination of the high doses of particulate. Additionally, while silica contributed to an increase in lymphocyte- and immune-related cytokines in the lungs (Tables 1–3), DPM reduced the expression of many proteins including: MIP-1α, GRO/KC, MIP-2, IL-2, IFN-γ, MMP-2 and MMP-9, in the BALF when in combination with silica, especially at early time points. DPM may exhibit independent action on macrophage activity, as well as lymphocyte influx and proliferation thus attenuating the effects induced on these cell types by silica alone (Tables 1–3). Immunological alterations were further examined by evaluating susceptibility to an infection following particulate exposure. While some alterations in immune cellular influx were observed in silica-exposed groups (Tables 5 and 6), the exposures did not alter the bacterial clearance rate or resolution of infection (Figure 4).

The toxicological properties of crystalline silica are well established. Silica is known to cause fibrotic changes in the lung following both acute exposures to bolus doses of particles and chronic lower dose exposure to particles (Castranova & Vallyathan, 2000). The mechanism directing the toxicity of silica particles in the lung still remains ambiguous but is thought to stem from multiple attributes relating to the crystalline structure of silica and its reactivity based on either surface charge or silicon-containing groups present on the surface of silica due to disruptions made to its structure during crushing, grinding and drilling (Castranova & Vallyathan, 2000). In conjunction with this, reactive oxygen/nitrogen species (ROS/RNS) associated with the particles themselves or as products of the respiratory

Table 5. Lymphocyte phenotype determination by flow cytometry in the BALF recovered from Sprague-Dawley rats exposed to DPM, SIL or DPM and SIL combined with LM.

	Exposure (μg)	Total lymphocytes	T cells	$CD4^+$ T cells	$CD8^+$ T cells	B cells
Day-1 postinfection	DPM 50	0.19 ± 0.22	−0.05 ± 0.20	−0.04 ± 0.20	−0.02 ± 0.27	0.17 ± 0.32
	SIL 233	0.92 ± 0.30@	0.90 ± 0.40	0.89 ± 0.37	0.88 ± 0.51	0.57 ± 0.40
	DS 50/233	0.52 ± 0.23	0.50 ± 0.26	0.48 ± 0.27	0.71 ± 0.38	0.09 ± 0.27
Day-3 postinfection	DPM 50	−0.07 ± 0.17	−0.31 ± 0.14	−0.17 ± 0.18	−0.35 ± 0.20	−0.15 ± 0.11
	SIL 233	−0.40 ± 0.15	−0.48 ± 0.09@	−0.30 ± 0.08	−0.53 ± 0.11	−0.40 ± 0.11
	DS 50/233	−0.54 ± 0.07	−0.59 ± 0.05@	−0.33 ± 0.07	−0.70 ± 0.04@	−0.60 ± 0.05@
Day-5 postinfection	DPM 50	0.001 ± 0.21	−0.04 ± 0.15	−0.18 ± 0.14	0.03 ± 0.16	0.34 ± 0.19
	SIL 233	−0.25 ± 0.17	−0.27 ± 0.13	−0.40 ± 0.10	−0.20 ± 0.14	−0.07 ± 0.24
	DS 50/233	−0.19 ± 0.21	−0.15 ± 0.24	−0.23 ± 0.14	−0.12 ± 0.31	−0.13 ± 0.15
Day-7 postinfection	DPM 50	−0.03 ± 0.12	0.05 ± 0.14	−0.02 ± 0.12	−0.004 ± 0.14	−0.13 ± 0.12
	SIL 233	−0.15 ± 0.10	−0.08 ± 0.13	−0.17 ± 0.10	−0.09 ± 0.17	0.10 ± 0.21
	DS 50/233	−0.20 ± 0.10	−0.19 ± 0.11	−0.27 ± 0.11	−0.17 ± 0.15	−0.21 ± 0.13
Day-14 postinfection	DPM 50	0.09 ± 0.14	0.17 ± 0.21	0.22 ± 0.25	0.18 ± 0.17	0.27 ± 0.26
	SIL 233	0.89 ± 0.20*	0.65 ± 0.23	1.01 ± 0.19	0.89 ± 0.36	−0.05 ± 0.12
	DS 50/233	0.95 ± 0.26*	0.80 ± 0.29	1.46 ± 0.54*	0.67 ± 0.23	0.002 ± 0.17

All data are shown as mean fold change over control ± standard error.
*Different from control and DPM 50 μg.
@Different from control. Statistical significance is $p \leq .05$.

Table 6. Lymphocyte phenotype determination by flow cytometry in the MLN excised from Sprague-Dawley rats exposed to DPM, SIL or DPM and SIL combined with LM.

	Exposure (μg)	Total lymphocytes	T cells	CD4+ T cells	CD8+ T cells	B cells
Day-1 postinfection	DPM 50	0.21 ± 0.21	0.18 ± 0.21	0.19 ± 0.20	0.12 ± 0.22	0.26 ± 0.23
	SIL 233	0.80 ± 0.26@	0.76 ± 0.24*	0.70 ± 0.22@	0.59 ± 0.22	0.69 ± 0.22
	DS 50/233	0.72 ± 0.18@	0.82 ± 0.19@	0.88 ± 0.19*	0.66 ± 0.18	0.66 ± 0.18
Day-3 postinfection	DPM 50	−0.16 ± 0.06	−0.18 ± 0.07	−0.08 ± 0.08	−0.30 ± 0.07@	−0.19 ± 0.06
	SIL 233	0.26 ± 0.10+	0.14 ± 0.09^	0.24 ± 0.10	−0.04 ± 0.08^	0.15 ± 0.09
	DS 50/233	−0.08 ± 0.08	−0.18 ± 0.03	−0.04 ± 0.02	−0.36 ± 0.04@	−0.03 ± 0.11
Day 5 postinfection	DPM 50	0.40 ± 0.16	0.35 ± 0.15	0.33 ± 0.15	0.38 ± 0.15	0.52 ± 0.22
	SIL 233	0.04 ± 0.10	0.03 ± 0.10	0.01 ± 0.10	0.04 ± 0.12	0.01 ± 0.09
	DS 50/233	0.32 ± 0.14	0.28 ± 0.13	0.28 ± 0.14	0.24 ± 0.12	0.37 ± 0.21
Day-7 postinfection	DPM 50	0.60 ± 0.27	0.72 ± 0.31	0.76 ± 0.31	0.66 ± 0.30	0.50 ± 0.25
	SIL 233	0.30 ± 0.20	0.34 ± 0.23	0.41 ± 0.25	0.24 ± 0.20	0.25 ± 0.18
	DS 50/233	0.40 ± 0.15	0.40 ± 0.16	0.47 ± 0.15	0.31 ± 0.19	0.40 ± 0.16
Day-14 postinfection	DPM 50	0.02 ± 0.28	−0.06 ± 0.27	−0.06 ± 0.27	−0.04 ± 0.29	0.18 ± 0.36
	SIL 233	0.03 ± 0.18	0.03 ± 0.19	0.01 ± 0.16	0.12 ± 0.26	0.12 ± 0.24
	DS 50/233	0.21 ± 0.26	0.21 ± 0.27	0.27 ± 0.30	0.15 ± 0.24	0.27 ± 0.31

All data are shown as mean fold change over control ± standard error.
*Different from control and DPM 50 μg.
@Different from control.
^Different from DPM 50 μg and DS 50/233 μg groups.
+Different from all other groups.
Statistical significance is $p \leq .05$.

burst following activation of phagocytes have been shown to drive a prolonged state of inflammation in the lungs (Blackford et al., 1994; Costa et al., 1991; Vallyathan et al., 1992, 1995). Studies investigating pulmonary toxicity of diesel demonstrate DPM-induced inflammation and oxidative stress as well (Bayram et al., 1998; Kim et al., 2016; Ohtoshi et al., 1998; Sagai et al., 1993, 1996); however, unlike silica, DPM exposure does not have the same propensity to cause fibrosis. Instead, chronic exposures to DE/DPM have been shown to cause disease outcomes including chronic obstructive pulmonary disorder, emphysema and cancer (Garshick et al., 2004; Hart et al., 2012; Kachuri et al., 2016; Wong et al., 1985).

In regards to potential mechanisms in the development of fibrosis, crystalline silica particles have been shown to either bind to scavenger receptors on alternatively activated macrophages (M2) followed by uptake into the cell in a phagosome, or the particles are phagocytosed by a classically activated macrophage (M1) in the interstitium once the M2 macrophages become overloaded (Kawasaki 2015). M2s are phenotypically distinct from M1s, being activated primarily by IL-4 and IL-13 rather than IFN-γ and are typically less involved in killing of microbes/clearance and more associated with functions of wound healing and collagen development (Mosser & Zhang, 2008). As reviewed by Kawasaki and demonstrated in original work by Joshi et al. (Fubini & Hubbard, 2003; Joshi et al., 2015; Kawasaki, 2015), the uptake of these particles triggers a signaling cascade within macrophages which leads to: the release of recruitment factors for additional inflammatory/immune cells, stimulation of the autocrine and paracrine production of fibrogenic mediators, and, most notably, either the successful clearance of particles from the lung to either the GI tract or lymphatics or the eventual phagolysosomal destruction and death of the cell that engulfed the particles. Directly following the death of a macrophage containing silica, the particles are engulfed by another nearby phagocyte. This repeated cycle of uptake, release and reuptake continues in the lung

until a point which cellular signals lead to the formation of a granuloma to sequester particles in an effort to reduce damage to the surrounding tissue (Dauber et al., 1980; Deshazo, 1982; Heppleston, 1982). It is hypothesized that M1-type macrophages may initiate this process (Kawasaki, 2015), but other cell types, including lymphocytes, epitheliod monocytes and macrophages and giant cells, are involved as well (Co et al., 2004; Langley et al., 2004; Prieditis & Adamson, 1996).

In relation to the fibrotic paradigm discussed above, this study showed that there were significant increases in neutrophil and lymphocyte recruitment in the high-dose coexposed group when compared to the silica-exposed group, along with significant increases in cytotoxicity in the lung measured as LDH in BALF, and this was accompanied by the increase in incidence of mild fibrosis at one-month postexposure in the high-dose coexposure group. While the interaction of silica with receptors was not investigated in the present study, downstream mediators of these interactions were increased in the BALF. Increases in chemotactic/recruitment proteins associated with inflammation (MCP-1, MIP-1α, RANTES, GRO/KC, MIP-2, IP-10 and TNF-α) were significantly increased in the groups containing the high dose of silica, and the increases tended to progress throughout the time course (Table 1), whereas the anti-inflammatory protein, IL-10, was significantly decreased in silica-exposed groups throughout the time course. Additionally, OPN, MMP-2 and MMP-9, proteins involved in tissue remodeling, were also significantly increased in silica-exposed groups, particularly later in the time course. Though differences between the high-dose coexposed group and high-dose silica-exposed group separately were not statistically significant for this parameter, there was approximately a 30% increase in MMP-9 expression, at the latest time point, suggesting a trend for increased tissue remodeling in the coexposed group over that of silica alone.

In addition to the pro-inflammatory responses discussed above, a significant increase in IL-18 at later time points following silica exposure was measured for both the high dose coexposed and high-dose silica only groups. The NLRP3 inflammasome is an immune system mediator that detects danger signals produced by damaged cells. The inflammasome is also activated by stimulation with foreign bioreactive particles like multiwalled carbon nanotubes, which cause production of oxidants by phagocytic cells leading to upregulation of NLRP3 complex formation, resulting in the cleavage of IL-18 and IL-1β and prolonged inflammation and fibrotic development in the lung (Gasse et al., 2009; Lee et al., 2016; Riteau et al., 2010; Sager et al., 2014; Sun et al., 2015). Crystalline silica exposure has also been shown to upregulate the activity of the NALP3/NLRP3 inflammasome following binding to scavenger receptors on macrophages both *in vitro* (Cassel et al., 2008; Dostert et al., 2008; Peeters et al., 2014) and *in vivo* (Peeters et al., 2014) leading to the cleavage of IL-1β and IL-18 to their active forms by caspases leading to apoptosis or pyroptosis in cells (Cassel et al., 2008; Iyer et al., 1996). While we did not observe an increase in IL-1β, we did observe an increase in IL-18 for both the SIL 233 and high-dose coexposed groups. At time points as early as one week following exposure, IL-18 was significantly increased in both groups compared with DPM 50, but by 3 months, both groups were significantly greater than both DPM 50 and control (Table 1). Therefore, inflammasome activation may also be occurring as an early response in the development of fibrosis.

In addition to the pro-inflammatory properties of both DPM and crystalline silica, both particles have been shown to alter mechanisms of pulmonary immunity, although the effects following exposure to these particles differ in this regard. Silica has been shown to cause hyper-activation and hyper-responsiveness of both macrophages (Castranova et al., 1985; Migliaccio et al., 2005) and T cells (Langley et al., 2004; Rocha-Parise et al., 2014). This was also demonstrated in the current study in the group exposed only to the high dose of silica individually. Conversely, DPM has been shown to suppress activation and effector functions of macrophages and T cells, and this suppression has been associated with increased susceptibility to infection and reduced pulmonary clearance of pathogens (Burchiel et al., 2004; Castranova et al., 1985; Mundandhara et al., 2006; Pierdominici et al., 2014; Yang et al., 1999, 2001; Yin et al. 2002, 2007). Because both DPM and silica exposure have been shown to increase lung inflammation and phagocytic recruitment in acute exposures but lead to decreased clearance following chronic exposure, it was of interest to determine whether the capacity for the clearance of a pathogen in an acute model of exposure to the particles in combination would be altered. In the present study, a difference in bacterial clearance from the lungs was not observed following exposure to DPM, silica, or the DPM and silica coexposure (Figure 4(A)); this may reflect the lower doses delivered here when compared to previous studies (Castranova et al., 2001; Cowie, 1994; Pasula et al., 2009; Sherson & Lander, 1990; Yang et al., 2001; Yin et al., 2002). Other differences among studies include the degree to which DPM or SIL were freshly collected, thus making them less reactive than particles that workers in the field may be exposed to (Castranova & Vallyathan, 2000; Dalal et al., 1990; Shoemaker et al., 1995), and the engine source of the DPM which would determine the elemental constituents. In addition, the timing of the infection may influence clearance of the infection following exposure. In studies in which a pathogenic response was examined more acutely (within 3 days of particle exposure), DPM exposure reduced clearance of the infection (Castranova et al., 2001; Yang et al., 2001; Yin et al., 2002). In response to silica exposure, clearance of bacteria has been shown to be critically dependent upon whether exposure is acute (Antonini et al., 2000), resulting in increased clearance of infection due to enhanced inflammatory and essentially a "primed" macrophage response for effective uptake and clearance of the bacteria, or chronic, resulting in decreased clearance (Cowie, 1994; Pasula et al., 2009; Sherson & Lander, 1990) suggesting the degree of lung injury present would alter susceptibility to infection. Further investigation is needed to determine the effects that particles might have on clearance and susceptibility to infections experienced more subsequently to particle exposure. Given that we observed development of fibrosis at later time

points, administering bacteria later in the time course, such as at 1, 2 or 3 months may result in more similar effects to what has been observed in chronic silica exposures previously (Cowie, 1994; Pasula et al., 2009; Sherson & Lander, 1990).

Conclusions

The data taken together show that DPM exposure at doses that do not elicit pulmonary toxicity has the capacity to significantly alter silica-induced pulmonary effects, primarily inflammation, oxidant production and rate of onset of fibrotic changes in the lung, as well as exhibit independent action which mediates some immune cell activity when the exposure occurs simultaneously as a mixture. The current study does not delineate the specific interactions between the two particulates in the lung following exposure and leading to the observed effects. One possibility is that presence of and/or injury induced by crystalline silica alters the clearance rate of the DPM particles from the lung, which in turn results in a longer persistence of DPM in the lung in conjunction with silica. DPM alone may be cleared at a greater rate resulting in the lack of observed toxicity following the individual exposures in this study. This hypothesis is supported by the evidence from the histopathology analysis in the observance of brown granules (DPM) in the lungs of only the coexposed group and by the presence of DPM particles in the lymph nodes of only the co-exposed group at the later time points and not the DPM-only exposure. Another possibility for the observed effects may be related to the particle load as a result of DPM and crystalline silica delivered to the lung simultaneously. Although the delivered doses by intratracheal instillation in these studies are lower than many previous studies (Antonini et al., 2000; Castranova et al., 2001; Pasula et al., 2009; Yang et al., 2001), the coexposed group received a total particle load of 283 µg compared to the individual silica load of 233 µg and the DPM load of 50 µg, which is an increase in load of ~18%. It is also important to note that though the doses are reflective of occupational settings and exposure over a period of time, intratracheal instillation does result in delivery of a bolus dose of particles rather than delivery of particles by inhalation at lower doses over time, which may affect the acute responses at the early time points postexposure instilling the particles ensure delivery of the entire dose to the lower respiratory tract of the lung, but overall is less physiological in nature than inhalation. Studies are underway to address doses administered as an intratracheal bolus and the effects of load and clearance in relationship to the combined exposure of DPM and silica.

Acknowledgements

The authors would like to acknowledge Rosana Schafer of the Department of Microbiology, Immunology, and Cell Biology at West Virginia University School of Medicine for her generous gift of *Listeria monocytogenes* (strain 10403 S, serotype 1).

Disclosure statement

No potential conflict of interest was reported by the authors.
Disclaimer: The findings and conclusions in this article are those of the author(s) and do not necessarily represent the view of the National Institute for Occupational Safety and Health.

Funding

This work was supported by National Institute for Occupational Safety and Health.

References

Abe S, Takizawa H, Sugawara I, Kudoh S. (2000). Diesel exhaust (DE)-induced cytokine expression in human bronchial epithelial cells: a study with a new cell exposure system to freshly generated DE in vitro. Am J Respir Cell Mol Biol. 22:296–303.

Antonini JM, Van Dyke K, Ye Z, et al. (1994). Introduction of luminol-dependent chemiluminescence as a method to study silica inflammation in the tissue and phagocytic cells of rat lung. Environ Health Perspect. 102 Suppl 10:37–42.

Antonini JM, Yang HM, Ma JY, et al. (2000). Subchronic silica exposure enhances respiratory defense mechanisms and the pulmonary clearance of Listeria monocytogenes in rats. Inhal Toxicol. 12:1017–36.

API. (2014). Oil and natural gas stimulate American economic and job growth. Online: American Petroleum Institute; Available from: http://www.api.org/~/media/Files/Policy/Jobs/Oil-Gas-Stimulate-Jobs-Economic-Growth/API-State-Vendor-Survey-Findings-Report.pdf.

Bayram H, Devalia JL, Sapsford RJ, et al. (1998). The effect of diesel exhaust particles on cell function and release of inflammatory mediators from human bronchial epithelial cells in vitro. Am J Respir Cell Mol Biol. 18:441–8.

Beamer CA, Holian A. (2008). Silica suppresses toll-like receptor ligand-induced dendritic cell activation. FASEB J. 22:2053–63.

Beatty TK, Shimshack JP. (2011). School buses, diesel emissions, and respiratory health. J Health Econ. 30:987–99.

Beckett W, Abraham J, Becklake M, et al. (1997). Adverse effects of crystalline silica exposure. Am J Respir Crit Care Med. 155:8.

Beckwith R. (2011). Proppants: where in the world. J Petrol Technol. 63:36–41.

Blackford JA, Jr., Antonini JM, Castranova V, Dey RD. (1994). Intratracheal instillation of silica up-regulates inducible nitric oxide synthase gene expression and increases nitric oxide production in alveolar macrophages and neutrophils. Am J Respir Cell Mol Biol. 11:426–31.

Brandt EB, Myers JMB, Acciani TH, et al. (2015). Exposure to allergen and diesel exhaust particles potentiates secondary allergen-specific memory responses, promoting asthma susceptibility. J Allergy Clin Immunol. 136:295–303.e7.

Brandt EB, Kovacic MB, Lee GB, et al. (2013). Diesel exhaust particle induction of IL-17A contributes to severe asthma. J Allergy Clin Immunol. 132:1194–204.e2.

Breitenstein M, Esswein EJ, Snawder J. (2011). NIOSH field effort to assess chemical exposures in oil and gas workers: health hazards in hydraulic fracturing. Proceedings of the NIOSH Intramural Science Conference.

Brown B. (2012). Hydrofrac sand in Wisconsin. University of Wisconsin Extension - Monroe County: WGaNH Survey.

Burchiel SW, Lauer FT, McDonald JD, Reed MD. (2004). Systemic immunotoxicity in AJ mice following 6-month whole body

inhalation exposure to diesel exhaust. Toxicol Appl Pharmacol. 196:337–45.
Cassel SL, Eisenbarth SC, Iyer SS, et al. (2008). The Nalp3 inflammasome is essential for the development of silicosis. Proc Natl Acad Sci USA. 105:9035–40.
Castranova V, Bowman L, Reasor MJ, et al. (1985). The response of rat alveolar macrophages to chronic inhalation of coal dust and/or diesel exhaust. Environ Res. 36:405–19.
Castranova V, Jones T, Barger M, et al. (1990). Pulmonary responses of guinea pigs to consecutive exposures to cotton dust. In: Jacobs R, Wakelyn P, Domelsmith L, (eds). Proceedings of the 14th Cotton Dust Research Conference; National Cotton Council.
Castranova V, Ma JY, Yang HM, et al. (2001). Effect of exposure to diesel exhaust particles on the susceptibility of the lung to infection. Environ Health Perspect. 109 Suppl 4:609–12.
Castranova V, Vallyathan V. (2000). Silicosis and coal workers' pneumoconiosis. Environ Health Perspect. 108 Suppl 4:675–84.
CDHS. (2002). Diesel engine exhaust health hazard advisory. In: Health hazard advisory California Department of Public Health: hazard evaluation system and information service; p. 1–6.
Certificate of Analysis Standard Reference Material 2975. (2013). Diesel particulate matter (Industrial Forklift). 2013 ed. Gaithersburg, MD: National Institute of Standards and Technology, US Department of Commerce; p. 11.
Co DO, Hogan LH, Il-Kim S, Sandor M. (2004). T cell contributions to the different phases of granuloma formation. Immunol Lett. 92:135–42.
Costa D, Fubini B, Giamello E, Volante M. (1991). A novel type of active site at the surface of crystalline SiO2(a-quartz) and its possible impact on pathogenicity. Can J Chem. 69:1427–34.
Cowie RL. (1994). The epidemiology of tuberculosis in gold miners with silicosis. Am J Respir Crit Care Med. 150:1460–2.
Creutzenberg O, Hansen T, Ernst H, et al. (2008). Toxicity of a quartz with occluded surfaces in a 90-day intratracheal instillation study in rats. Inhal Toxicol. 20:995–1008.
Dalal NS, Shi XL, Vallyathan V. (1990). ESR spin trapping and cytotoxicity investigations of freshly fractured quartz: mechanism of acute silicosis. Free Radic Res Commun 9:259–66.
Dauber JH, Rossman MD, Pietra GG, et al. (1980). Experimental silicosis: morphologic and biochemical abnormalities produced by intratracheal instillation of quartz into guinea pig lungs. Am J Pathol. 101:595–612.
Deshazo R. (1982). Current concepts about the pathogenesis of silicosis and asbestosis. J. Allergy Clin Immunol. 70:41–9.
Diaz-Sanchez D, Garcia MP, Wang M, et al. (1999). Nasal challenge with diesel exhaust particles can induce sensitization to a neoallergen in the human mucosa. J Allergy Clin Immunol. 104:1183–8.
Dostert C, Petrilli V, Van Bruggen R, et al. (2008). Innate immune activation through Nalp3 inflammasome sensing of asbestos and silica. Science (New York, NY). 320:674–7.
Esswein EJ, Breitenstein M, Snawder J, et al. (2013). Occupational exposures to respirable crystalline silica during hydraulic fracturing. J Occup Environ Hyg. 10:347–56.
Fubini B, Hubbard A. (2003). Reactive oxygen species (ROS) and reactive nitrogen species (RNS) generation by silica in inflammation and fibrosis. Free Radic Biol Med. 34:1507–16.
Garshick E, Laden F, Hart JE, et al. (2004). Lung cancer in railroad workers exposed to diesel exhaust. Environ Health Perspect. 12:1539–43.
Gasse P, Riteau N, Charron S, et al. (2009). Uric acid is a danger signal activating NALP3 inflammasome in lung injury inflammation and fibrosis. Am J Respir Crit Care Med. 179:903–13.
Gauderman WJ, Avol E, Gilliland F, et al. (2004). The effect of air pollution on lung development from 10 to 18 years of age. N Engl J Med. 351:1057–67.
Ghio AJ, Jaskot RH, Hatch GE. (1994). Lung injury after silica instillation is associated with an accumulation of iron in rats. Am J Physiol. 267:L686–92.
Ghio AJ, Smith CB, Madden MC. (2012a). Diesel exhaust particles and airway inflammation. Curr Opin Pulm Med. 18:144–50.
Ghio AJ, Sobus JR, Pleil JD, Madden MC. (2012b). Controlled human exposures to diesel exhaust. Swiss Med Wkly. 142:w13597.
Gwinn MR, Leonard SS, Sargent LM, et al. (2009). The role of p53 in silica-induced cellular and molecular responses associated with carcinogenesis. J Toxicol Environ Health A. 72:1509–19.
Hart JE, Eisen EA, Laden F. (2012). Occupational diesel exhaust exposure as a risk factor for chronic obstructive pulmonary disease. Curr Opin Pulm Med. 18:151–4.
Heppleston AG. (1982). Silicotic fibrogenesis: a concept of pulmonary fibrosis. Ann Occup Hyg. 26:449–62.
Hesterberg TW, Long CM, Bunn WB, et al. (2009). Non-cancer health effects of diesel exhaust: a critical assessment of recent human and animal toxicological literature. Crit Rev Toxicol. 39:195–227.
Hnizdo E. (2003). Chronic obstructive pulmonary disease due to occupational exposure to silica dust: a review of epidemiological and pathological evidence. Occup Environ Med. 60:237–43.
Huaux F, Louahed J, Hudspith B, et al. (1998). Role of interleukin-10 in the lung response to silica in mice. Am J Respir Cell Mol Biol. 18:51–9.
HSE. (2012). Control of diesel engine exhaust emissions in the workplace. In: HSG187. 3rd ed. London, UK: Crown Copyright. p. 1–21.
IARC. (2012). Online/lancet: World Health Organization: International Agency for Research on Cancer.
Ichinose T, Furuyama A, Sagai M. (1995). Biological effects of diesel exhaust particles (DEP). II. Acute toxicity of DEP introduced into lung by intratracheal instillation. Toxicology. 99:153–67.
ICRP. (1994). Human respiratory tract model for radiological protection: a report of a task group of the International Commission on Radiological Protection. Ann ICRP. 24:1–482.
Iyer R, Hamilton RF, Li L, Holian A. (1996). Silica-induced apoptosis mediated via scavenger receptor in human alveolar macrophages. Toxicol Appl Pharmacol. 141:84–92.
Joshi GN, Goetjen AM, Knecht DA. (2015). Silica particles cause NADPH oxidase-independent ROS generation and transient phagolysosomal leakage. Mol Biol Cell. 26:3150–64.
Jung EJ, Avliyakulov NK, Boontheung P, et al. (2007). Pro-oxidative DEP chemicals induce heat shock proteins and an unfolding protein response in a bronchial epithelial cell line as determined by DIGE analysis. Proteomics. 7:3906–18.
Kachuri L, Villeneuve PJ, Parent ME, et al. (2014). Occupational exposure to crystalline silica and the risk of lung cancer in Canadian men. Int J Cancer. 135:138–48.
Kachuri L, Villeneuve PJ, Parent ME, et al. (2016). Workplace exposure to diesel and gasoline engine exhausts and the risk of colorectal cancer in Canadian men. Environ Health. 15:4.
Kajiwara T, Ogami A, Yamato H, et al. (2007). Effect of particle size of intratracheally instilled crystalline silica on pulmonary inflammation. J Occup Health. 49:88–94.
Kawasaki H. (2015). A mechanistic review of silica-induced inhalation toxicity. Inhal Toxicol. 27:363–77.
Kim BG, Lee PH, Lee SH, et al. (2016). Long-term effects of diesel exhaust particles on airway inflammation and remodeling in a mouse model. Allergy Asthma Immunol Res. 8:246–56.
Langley RJ, Kalra R, Mishra NC, et al. (2004). A biphasic response to silica: I. Immunostimulation is restricted to the early stage of silicosis in lewis rats. Am J Respir Cell Mol Biol. 30:823–9.
Le Vee M, Jouan E, Lecureur V, Fardel O. (2016). Aryl hydrocarbon receptor-dependent up-regulation of the heterodimeric amino acid transporter LAT1 (SLC7A5)/CD98hc (SLC3A2) by diesel exhaust particle extract in human bronchial epithelial cells. Toxicol Appl Pharmacol. 290:74–85.
Lee S, Suh GY, Ryter SW, Choi AM. (2016). Regulation and function of the nucleotide binding domain leucine-rich repeat-containing receptor, pyrin domain-containing-3 inflammasome in lung disease. Am J Respir Cell Mol Biol. 54:151–60.
Liao CM, Wu BC, Cheng YH, et al. (2015). Ceramics manufacturing contributes to ambient silica air pollution and burden of lung disease. Environ Sci Pollut Res Int. 22:15067–79.
Liu Y, Rong Y, Steenland K, et al. (2014). Long-term exposure to crystalline silica and risk of heart disease mortality. Epidemiology (Cambridge, Mass). 25:689–96.

Lucking AJ, Lundback M, Barath SL, et al. (2011). Particle traps prevent adverse vascular and prothrombotic effects of diesel engine exhaust inhalation in men. Circulation. 23:1721–8.

Ma JY, Ma JK. (2002). The dual effect of the particulate and organic components of diesel exhaust particles on the alteration of pulmonary immune/inflammatory responses and metabolic enzymes. J Environ Sci Health C Environ Carcinog Ecotoxicol Rev. 20:117–47.

Ma JY, Young SH, Mercer RR, et al. (2014). Interactive effects of cerium oxide and diesel exhaust nanoparticles on inducing pulmonary fibrosis. Toxicol Appl Pharmacol. 278:135–47.

Maciejewska A. (2014). Health effects of occupational exposure to crystalline silica in the light of current research results. Medycyna Pracy. 65:799–818.

Madden MC, Richards JH, Dailey LA, et al. (2000). Effect of ozone on diesel exhaust particle toxicity in rat lung. Toxicol Appl Pharmacol. 68:140–8.

Madl AK, Donovan EP, Gaffney SH, et al. (2008). State-of-the-science review of the occupational health hazards of crystalline silica in abrasive blasting operations and related requirements for respiratory protection. J Toxicol Environ Health B Crit Rev. 11:548–608.

Mauderly JL, Snipes MB, Barr EB, et al. (1994). Pulmonary toxicity of inhaled diesel exhaust and carbon black in chronically exposed rats. Part I: neoplastic and nonneoplastic lung lesions. Res Rep. 1994/10:1–75. discussion 77–97.

McCreanor J, Cullinan P, Nieuwenhuijsen MJ, et al. (2007). Respiratory effects of exposure to diesel traffic in persons with asthma. N Engl J Med. 57:2348–58.

McDonald JD, Zielinska B, Sagebiel JC, McDaniel MR. (2002). Characterization of fine particle material in ambient air and personal samples from an underground mine. Aerosol Sci Tech. 36:1033–44.

Mercer RR, Russell ML, Crapo JD. (1994). Alveolar septal structure in different species. J Appl Physiol. 77:1060–6.

Migliaccio CT, Hamilton RF, Jr, Holian A. (2005). Increase in a distinct pulmonary macrophage subset possessing an antigen-presenting cell phenotype and in vitro APC activity following silica exposure. Toxicol Appl Pharmacol. 205:168–76.

Mosser DM, Zhang X. (2008). Activation of murine macrophages. Curr Protoc Immunol. 83:14.2.1–14.2.8.

Mundandhara SD, Becker S, Madden MC. (2006). Effects of diesel exhaust particles on human alveolar macrophage ability to secrete inflammatory mediators in response to lipopolysaccharide. Toxicol In Vitro. 20:614–24.

Nightingale JA, Maggs R, Cullinan P, et al. (2000). Airway inflammation after controlled exposure to diesel exhaust particulates. Am J Respir Crit Care Med. 162:161–6.

Ohtoshi T, Takizawa H, Okazaki H, et al. (1998). Diesel exhaust particles stimulate human airway epithelial cells to produce cytokines relevant to airway inflammation in vitro. J Allergy Clin Immunol. 101:778–85.

OSHA/MSHA. 2013. Diesel exhaust/diesel particulate matter. United States Department of Labor. Available from: https://www.osha.gov/dts/hazardalerts/diesel_exhaust_hazard_alert.html. [Last accessed: 07 Aug 2017].

Ovrevik J, Lag M, Schwarze P, Refsnes M. (2004). p38 and Src-ERK1/2 pathways regulate crystalline silica-induced chemokine release in pulmonary epithelial cells. Toxicol Sci. 81:480–90.

OSHWiki Contributors. 2017. Workplace exposure to dusts and aerosols – diesel exhaust [Internet]. OSHWiki; 2017 May 30, 15:01 UTC. Available from: https://oshwiki.eu/index.php?title=Workplace_exposure_to_dusts_and_aerosols_-_diesel_exhaust&oldid=247433. [Last accessed: 2 Aug 2017].

Pasula R, Britigan BE, Turner J, Martin WJ. 2nd. (2009). Airway delivery of silica increases susceptibility to mycobacterial infection in mice: potential role of repopulating macrophages. J Immunol. 182:7102–9.

Peeters PM, Eurlings IM, Perkins TN, et al. (2014). Silica-induced NLRP3 inflammasome activation in vitro and in rat lungs. Part Fibre Toxicol. 11:58.

Pierdominici M, Maselli A, Cecchetti S, et al. (2014). Diesel exhaust particle exposure in vitro impacts T lymphocyte phenotype and function. Part Fibre Toxicol. 11:74.

Porter DW, Ye J, Ma J, et al. (2002). Time course of pulmonary response of rats to inhalation of crystalline silica: NF-kappa B activation, inflammation, cytokine production, and damage. Inhal Toxicol. 14:349–67.

Prieditis H, Adamson IY. (1996). Alveolar macrophage kinetics and multinucleated giant cell formation after lung injury. J Leukoc Biol. 59:534–8.

Pronk A, Coble J, Stewart PA. (2009). Occupational exposure to diesel engine exhaust: a literature review. J Expo Sci Environ Epidemiol. 19:443–57.

Provoost S, Maes T, Willart MA, et al. (2010). Diesel exhaust particles stimulate adaptive immunity by acting on pulmonary dendritic cells. J Immunol. 184:426–32.

QDNRM. (2014). Guidance note for management of diesel engine exhuast in metalliferous mines. In: QGN 21. 1st ed. Mining and Quarrying Safety and Health Act of 1999. Australia: Queensland Government; p. 1–26.

Riteau N, Gasse P, Fauconnier L, et al. (2010). Extracellular ATP is a danger signal activating P2X7 receptor in lung inflammation and fibrosis. Am J Respir Crit Care Med. 182:774–83.

Roberts RR, Mercer RR, Chapman RS, et al. (2012). Pulmonary toxicity, distribution, and clearance of intratracheally instilled silicon nanowires in rats. J Nanomater. 12:17.

Robertson S, Gray GA, Duffin R, et al. (2012). Diesel exhaust particulate induces pulmonary and systemic inflammation in rats without impairing endothelial function ex vivo or in vivo. Part Fibre Toxicol. 9:9.

Rocha-Parise M, Santos LM, Damoiseaux JG, et al. (2014). Lymphocyte activation in silica-exposed workers. Int J Hyg Environ Health. 17:586–91.

Sagai M, Furuyama A, Ichinose T. (1996). Biological effects of diesel exhaust particles (DEP). III. Pathogenesis of asthma like symptoms in mice. Free Radic Biol Med. 21:199–209.

Sagai M, Saito H, Ichinose T, et al. (1993). Biological effects of diesel exhaust particles. I. in vitro production of superoxide and in vivo toxicity in mouse. Free Radic Biol Med. 14:37–47.

Sager TM, Wolfarth MW, Andrew M, et al. (2014). Effect of multi-walled carbon nanotube surface modification on bioactivity in the C57BL/6 mouse model. Nanotoxicology. 8:317–27.

Salvi S, Blomberg A, Rudell B, et al. (1999). Acute inflammatory responses in the airways and peripheral blood after short-term exposure to diesel exhaust in healthy human volunteers. Am J Respir Crit Care Med. 159:702–9.

Satpathy SR, Jala VR, Bodduluri SR, et al. (2015). Crystalline silica-induced leukotriene B4-dependent inflammation promotes lung tumour growth. Nat Commun. 6:7064.

Sellamuthu R, Umbright C, Li S, et al. (2011). Mechanisms of crystalline silica-induced pulmonary toxicity revealed by global gene expression profiling. Inhal Toxicol. 223:927–37.

Sellamuthu R, Umbright C, Roberts JR, et al. (2013). Molecular insights into the progression of crystalline silica-induced pulmonary toxicity in rats. J Appl Toxicol. 33:301–12.

Sherson D, Lander F. (1990). Morbidity of pulmonary tuberculosis among silicotic and nonsilicotic foundry workers in Denmark. J Occup Med. 32:110–13.

Shi X, Mao Y, Danie LN, et al. (1995). Generation of reactive oxygen species by quartz particles and its implication for cellular damage. Appl Occup Environl Hyg. 10:1138–44.

Shoemaker DA, Pretty JR, Ramsey DM, et al. (1995). Particle activity and in vivo pulmonary response to freshly milled and aged alpha-quartz. Scand J Work Environ Health. 21 Suppl 2:15–18.

Siegel PD, Saxena RK, Saxena QB, et al. (2004). Effect of diesel exhaust particulate (DEP) on immune responses: contributions of particulate versus organic soluble components. J Toxicol Environ Health Part A. 67:221–31.

Singh P, DeMarini DM, Dick CA, et al. (2004). Sample characterization of automobile and forklift diesel exhaust particles and comparative pulmonary toxicity in mice. Environ Health Perspect. 112:820–5.

Steerenberg PA, Zonnenberg JA, Dormans JA, et al. (1998). Diesel exhaust particles induced release of interleukin 6 and 8 by (primed) human bronchial epithelial cells (BEAS 2B) in vitro. Exp Lung Res. 24:85–100.

Sun B, Wang X, Ji Z, et al. (2015). NADPH oxidase-dependent NLRP3 inflammasome activation and its important role in lung fibrosis by multiwalled carbon nanotubes. Small. 11:2087–97.

SUVA DoOM. (2013). Grenzwerte am Arbeitsplatz. In: 1903d online: SUVA. p. 1–150. Database Name 2013. Lucerne, Switzerland: OSHwiki. Available from: https://oshwiki.eu/wiki/Workplace_exposure_to_dusts_and_aerosols_-_diesel_exhaust.

TERA. (2014). Occupational exposure limit evaluation: diesel particulate matter. 9 October 2014. Cincinnati, OH: Toxicology Excellence for Risk Assessment.

Tomaru M, Matsuoka M. (2011). The role of mitogen-activated protein kinases in crystalline silica-induced cyclooxygenase-2 expression in A549 human lung epithelial cells. Toxicol Mech Methods. 21:513–9.

Totlandsdal AI, Lag M, Lilleaas E, et al. (2015). Differential proinflammatory responses induced by diesel exhaust particles with contrasting PAH and metal content. Environ Toxicol. 30:188–96.

Underwood E. (1970). Quantitative stearology. Philippines: Addison-Wesley Publishing Company.

Vallyathan V, Castranova V, Pack D, et al. (1995). Freshly fractured quartz inhalation leads to enhanced lung injury and inflammation. Potential role of free radicals. Am J Respir Crit Care Med. 152:1003–9.

Vallyathan V, Mega JF, Shi X, Dalal NS. (1992). Enhanced generation of free radicals from phagocytes induced by mineral dusts. Am J Respir Cell Mol Biol. 6:404–13.

Vattanasit U, Navasumrit P, Khadka MB, et al. (2014). Oxidative DNA damage and inflammatory responses in cultured human cells and in humans exposed to traffic-related particles. Int J Hygiene Environ Health. 17:23–33.

Wong O, Morgan RW, Kheifets L, et al. (1985). Mortality among members of a heavy construction equipment operators union with potential exposure to diesel exhaust emissions. British journal of industrial. Medicine. 42:435–48.

Yang HM, Antonini JM, Barger MW, et al. (2001). Diesel exhaust particles suppress macrophage function and slow the pulmonary clearance of Listeria monocytogenes in rats. Environ Health Perspect. 109:515–21.

Yang HM, Barger MW, Castranova V, et al. (1999). Effects of diesel exhaust particles (DEP), carbon black, and silica on macrophage responses to lipopolysaccharide: evidence of DEP suppression of macrophage activity. J Toxicol Environ Health. 58:261–78.

Yassin A, Yebesi F, Tingle R. (2005). Occupational exposure to crystalline silica dust in the United States, 1988-2003. Environ Health Perspect. 113:255–60.

Yin XJ, Dong CC, Ma JY, et al. (2007). Suppression of phagocytic and bactericidal functions of rat alveolar macrophages by the organic component of diesel exhaust particles. J Toxicol Environ Health A. 70:820–8.

Yin XJ, Schafer R, Ma JY, et al. (2002). Alteration of pulmonary immunity to Listeria monocytogenes by diesel exhaust particles (DEPs). I. Effects of DEPs on early pulmonary responses. Environ Health Perspect. 110:1105–11.

Zhao H, Ma JK, Barger MW, et al. (2009). Reactive oxygen species- and nitric oxide-mediated lung inflammation and mitochondrial dysfunction in wild-type and iNOS-deficient mice exposed to diesel exhaust particles. J Toxicol Environ Health Part A. 72:560–70.

Zhou F, Li S, Jia W, et al. (2015). Effects of diesel exhaust particles on microRNA-21 in human bronchial epithelial cells and potential carcinogenic mechanisms. Mol Med Rep. 12:2329–35.